Photoaffinity Labels of Daptomycin

by

Joshua Williams

A thesis

presented to the University of Waterloo

in fulfillment of the

thesis requirement for the degree of

Master of Applied Science

in

Chemistry

Waterloo, Ontario, Canada, 2014

Author's Declaration

I hereby declare that I am the sole author of this thesis. This is a true copy of the thesis, including any required final revisions, as accepted by my examiners.

I understand that my thesis may be made electronically available to the public.

Abstract

Daptomycin (Dap) is a cyclic lipodepsipeptide antibiotic that is currently used in the treatment of bacterial infections caused by *Staphylococcus aureus* including the strains that are methicillin-resistant (MRSA), as well as vancomycin-resistant (VRSA). Although it is known that daptomycin inserts into the membrane of the bacteria causing cell death very few details of its specific mechanism of action have been elucidated. Studies on Dap-resistant bacteria suggest that Dap may interact with specific proteins as well as specific lipids. It is anticipated that a photoaffinity label (PAL) of daptomycin (Dap-PAL) will be useful in determining what bacterial membrane components interact with Dap. The objective of this proposal is to prepare a photoaffinity label of daptomycin. Starting from 4,4'-dimethylbenzophenone, a benzophenone derivative was prepared that contained a 4-aldehyde moiety and a 4'-alkyl tail which contained a terminal alkyne group. This derivative was attached to the Orn residue in Dap via reductive amination to give the desired Dap-PAL. The minimal inhibitory concentration (MIC) of the Dap-PAL with *Bacillus subtillus* was determined to be 1.5 μg/mL which is only two times greater than the MIC of Dap.

Acknowledgements

I would like to express my thanks to my supervisor, Dr. Scott Taylor, for his guidance and encouragement. I am grateful to the members of my committee, Dr. Gary Dmitrienko, and Dr. John Honek. I would like to give a special thanks to the Taylor lab members for their assistance. I would also like to thank my family and friends for their support, and encouragement.

Table of Contents

List of Figures

Chapter 1 - Daptomycin and Photoaffinty Labeling

Chapter 2 - Synthesis of a Daptomycin Photoaffinity Label

List of Schemes

Chapter 2 - Synthesis of a Daptomycin Photoaffinity Label

List of Abbreviations

Abbreviations	Full Name
ACP	Acyl Carrier Protein
AIBN	Azobisisobutyronitrile
BP	Benzophenone
CPK	Creatine phosphokinase
Dap	Daptomycin
Dap-PAP	Daptomycin Photoaffinity Probe
DMF	Dimethylformamide
FA	Fatty Acid
FRET	Fluorescence Resonance Energy Transfer
HPLC	High Performance Liquid Chromatography
Ile	Isoleucine
Kyn	Kyneurinine
LPG	Lysyl phosphatidylglycerol
MeGlu	Methyl Glutamic Acid
MIC	Minimum Inhibitory Concentration
mprF	Multiple Peptide resistance Factor
MRSA	Methicillin Resistant *Staphylococcus aureus*
MS	Mass Spectrometry
NBS	N-bromosuccinimide
NMR	Nuclear Magnetic Resonance
NRPS	Nonribosomal Peptide Synthases
Orn	Ornithine

PAL	Photoaffinity Labelling
PAP	Photoaffinity Probe
PCC	Pyridinium chlorochromate
PD_{50}	Concentration required to protect 50% of the animals challenged
PG	Phospatidylglycerol
SAR	Structure Activity Relationship
STAB-H	Sodium triacetoxyborohydride
TE	Thioesterase
TFA	Trifluoroacetic acid
THF	Tetrahydrofuran
TMS	Tetramethylsilane
VRSA	Vancomycin Resistant *Staphylococcus aureus*
UV	Ultraviolet

Chapter 1 – Daptomycin and Photoaffinity Labeling

1.1 Classical Antibiotics:

Not counting our immune system, antibiotics are our main defence against bacterial infections. The most common and widely used class of antibiotics are the β-lactams. They function by inhibiting bacterial cell wall synthesis.[1] These compounds, an example of which is penicillin (figure 1.1), are often the first choice of physicians when treating bacterial infections.[1] Soon after the introduction of penicillin, resistant strains of *Staphylococcus aureus*, a Gram-positive bacterium that produces β-lactamase, an enzyme that destroys penicillin by catalyzing hydrolysis of the β-lactam, were discovered.[1] Methicillin (figure. 1.1), a semi-synthetic β-lactam antibiotic that is much less susceptible to β-lactamases was developed, but soon methicillin-resistant strains of *S. aureus* (MRSA) were discovered.[1] Methicillin resistance is a major challenge today, and this very serious problem is currently being tackled by many research groups worldwide. Glycopeptides, such as vancomycin (figure 1.1), which inhibit cell wall synthesis but by a mechanism different from that of the β-lactams, are now used as the stand-by drugs for treating MRSA.[1] However, in 1996 strains of vancomycin resistant *S. aureus* (VRSA) were discovered.[2] This was very alarming as vancomycin was considered to be the ultimate weapon when combating MRSA.

Many different approaches have been taken to combat antibiotic resistance. An obvious tactic is to develop antibiotics that target cell functions other than just cell wall biosynthesis.[1] However, the inhibition of cell wall growth is still the most common and effective approach to generating antibiotics, and these methods are still being actively explored. Cell wall synthesis is very well understood, and the drugs made to combat cell wall synthesis of bacteria are usually less toxic to humans due to the lack of a cell wall in mammalian cells. Despite this, a new mode of

action is still desirable due to the emergence of bacterial that are resistant to the current methods of treatment such as MRSA and VRSA.

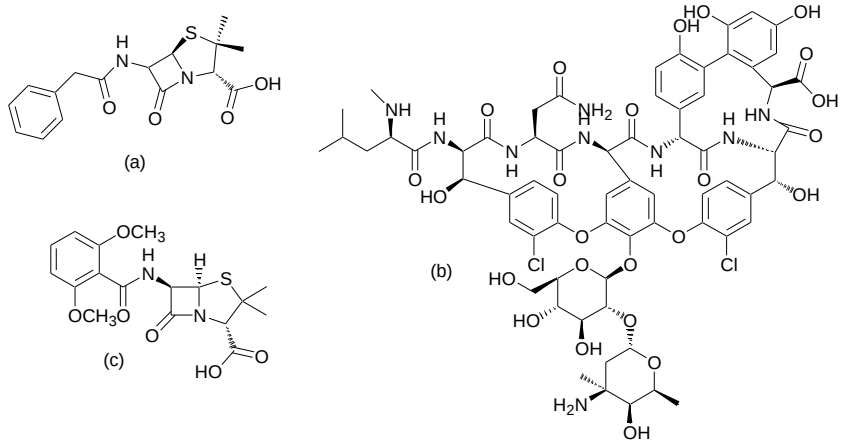

Figure 1.1: Classical antibiotic structures: (a) Penicillin, (b) Vancomycin, (c) Methicillin

1.2 Daptomycin

1.2.1 History

Daptomycin (Dap) is a 10-membered cyclic lipopeptide antibiotic (figure 1.2). It contains six non-proteinogenic amino acids (D-asparagine, D-alanine, D-serine, ornithine, (2S,3R)-3-methyl-glutamic acid and kynurenine), and an N-terminus that is acylated with an n-decanoyl fatty acid side chain (figure 1.2). Dap was discovered in the early 1980s by scientists at Eli Lilly from a soil sample from Mount Ararat in Turkey.[3] Dap is a natural product of a soil actinomycete, just like most important antibiotics from the last 50 years.[4] This actinomycete, known as *Streptomyces roseosporus*, produced a family of lipopeptides which were given the designation A21987C by Eli Lilly.[3] Along with the discovery of *S. roseosporus*, these scientists also isolated a deacylase gene that was secreted from *Actinoplanes utahensis*, which was able to cleave the long lipid side chain from the tryptophan residue of A21987C.[5,6] From this, the peptide core of the A21987C family

was isolated, and reacylated with different side chains. Dap, which contains an n-decanoyl side chain, was chosen for clinical trials due to the fact that it had good antibacterial properties and exhibited low toxicity in animals.[3] The process of deacylation followed by reacylation was time consuming and cost-ineffective. To deal with this, the scientists at Eli Lilly developed a method in which decanoic acid was fed into to *S. roseosporus* during the fermentation process, which would directly produce only Dap rather than a mixture of different A21987C members.

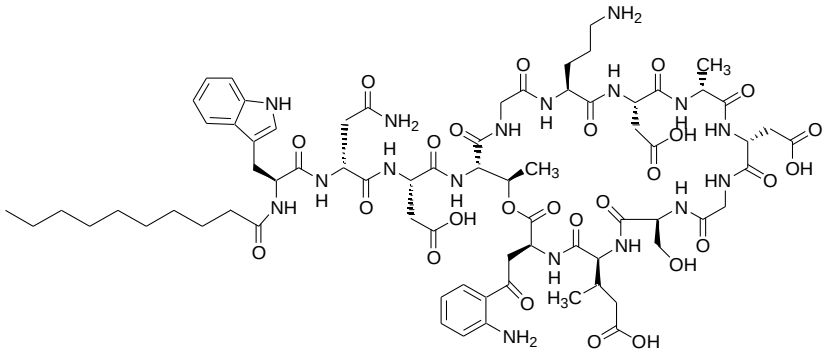

Figure 1.2: Daptomycin

The scientists at Eli Lilly began clinical trials of Dap through intravenous delivery in the early 1990s.[7] Dap was tolerated by all human volunteers when given in 0.5-6 mg/kg doses, once daily.[7] However, in phase II trials, which involved giving volunteers 4 mg/kg doses twice daily, the volunteers began to experience muscle pain as well as elevated creatine phosphokinase (CPK) levels, all of which subsided upon discontinuation of use.[8] Upon discovering this, Eli Lilly shut down the research on Dap.

Cubist Pharmaceuticals purchased the rights to Dap from Eli Lilly in 1997.[9] They found that it was the treatment interval, not the Dap concentration which was causing the muscle toxicity and higher CPK levels.[10] They found that the side effects reported by Eli Lily could be minimized by employing a dose regimen that was different from the one used by Eli Lily. Cubist patented

this method in 2002. The FDA approved Dap for use against severe skin infections caused by Gram-positive bacteria including methicillin resistant *Staphylococcus aureus* (MRSA) and vancomycin resistant *Staphylococcus aureus* (VRSA) as well as right-sided endocarditis in 2006. Dap is marketed under the trade name Cubicin®.[9]

1.2.2 Biosynthesis of Daptomycin

In *S. roseosporus*, the biosynthesis of Dap is controlled by three nonribosomal peptide synthases (NRPS), which are DptA, DptBC, and DptD, as well as trans acting enzymes.[11,12,13] This is highlighted in figure 1.3. The construction of the Dap molecule is done using a thiotemplate-directed approach.[14] The multidomain of the NRPS can be further classified into modules and domains.[15,16] Each and every module takes care of the specific recognition, activation, binding and incorporation of another building block onto the ogliopeptide.[17] The first step that takes place in the biosynthesis is the acylation of the terminal amino acid, which in this case is tryptophan. This is done when an acyl-CoA ligase activates the fatty acid (FA), as well as the acyl carrier protein (ACP) that the FA will be covalently tethered to.[11] The N-terminal C domain catalyzes the condensation between tryptophan and the FA.[18] The initiation of the biosynthesis is helped by two enzymes called DptE and DptF.[14] DptE activates the FA attached to the N-terminus of Dap in an ATP-dependant manner.[14] The activated FA is then transferred to DptF. The N-terminal of the C-domain of the DptA initiation module then catalyzes the condensation between the ACP bound FA and tryptophan.[14] DptE has a very diverse substrate tolerance, which is why the A21978C family has so many different members.[14]

After the initiation of the synthesis, the amino acid chain is elongated by linearly operating NRPSs, DptA, DptBC, and DptD.[11] It should be noted that aside from the important ornithine and

kynurenine residues, there is also the methyl-glutamic acid residue (MeGlu) that is incorporated into the ring.[19] MeGlu contributes to the biological activity of Dap, and is located at the same spot in many other peptide rings in different lipopeptide antibiotics.[19,20,21] Once the peptide chain has been completed, it encounters the thioesterase (TE) domain, which is located in DptD. This TE domain promotes the intramolecular attack of the hydroxyl group of threonine on the acyl-O-TE oxoester intermediate, which will lead to the release of the cyclic lipopeptide.[21]

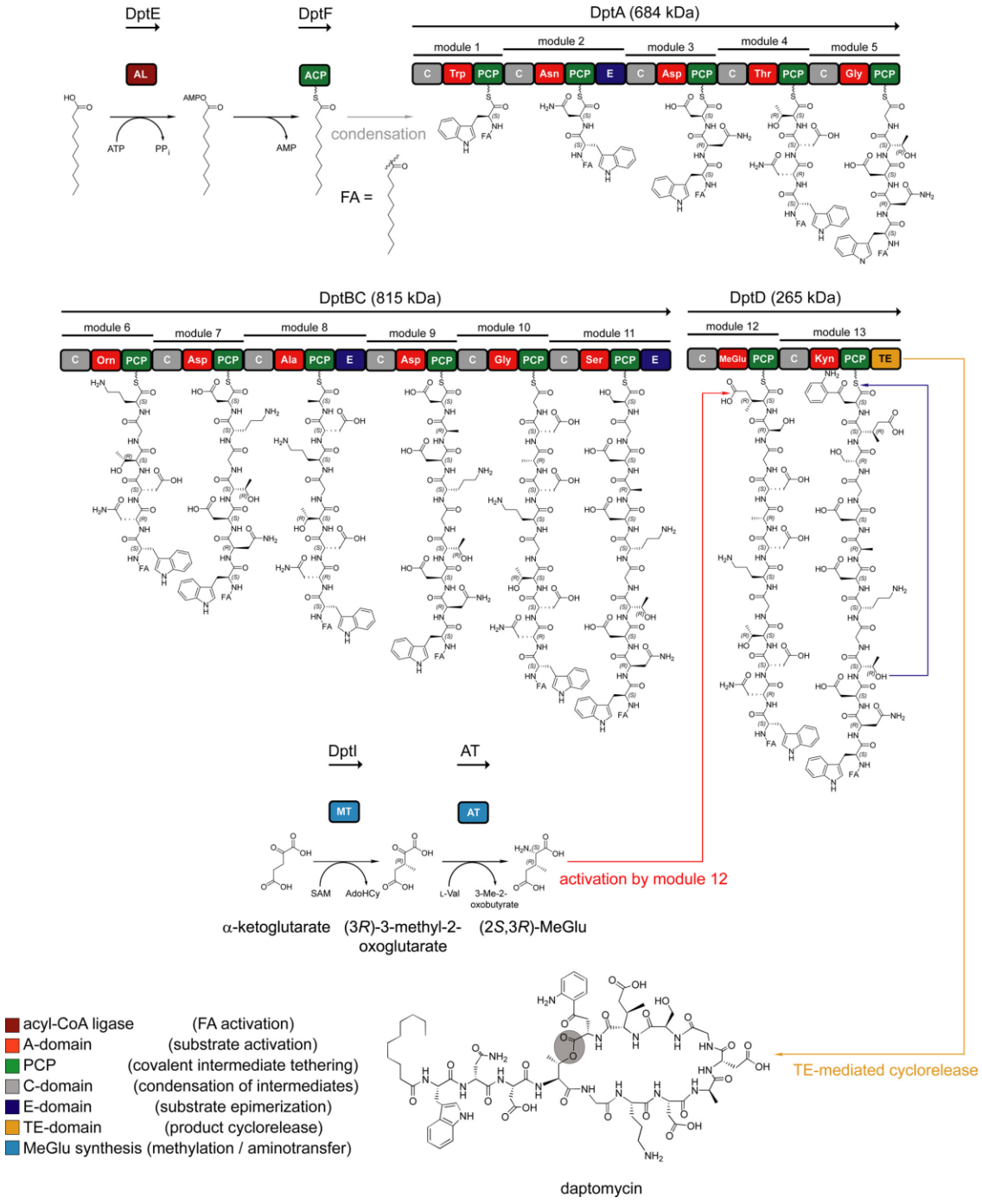

Figure 1.3: Schematic overview of Dap biosynthesis by *S. roseosporus*. Taken with permission from reference 14.

1.2.3 Mechanism of Action

The mechanism of action of Dap is not very well understood. It was demonstrated shortly after its discovery that removing the hydrophobic acyl chain results in complete loss of antibiotic activity leading to the proposition that the tail inserts into the bacterial membrane and this insertion is essential for activity. Dap activity correlates with the target membrane's content of phosphatidylglycerol (PG). Dap activity is dependent on Ca^{+2} ions and reaches its maximum antibacterial potency at Ca^{+2} concentrations of 1.25 mM, which is similar to the concentration of ionized calcium in human serum.[22] The vast majority of mechanistic studies have been performed using model membrane systems (micelles, liposomes). Nevertheless, these studies yielded some important information. NMR studies in the absence of model or bacterial membranes demonstrated a 1:1 stoichiometry of Dap:Ca^{+2} binding.[23] It has been proposed that the Ca^{+2} ions mask the negative charges on Dap and act as a bridge between the head groups of Dap and acidic phospholipids in the cell membrane.[24] On the basis of NMR studies, Ho *et al* have suggested that Dap forms micelles consisting of 14–16 monomers upon addition of Ca^{+2} at a 1:1 ratio.[25] These workers proposed a mechanism of action for which Dap, upon binding Ca^{+2} ions, forms micelles consisting of 14-16 monomers which then deliver Dap to the bacterial cell membranes in high local concentrations and a functional conformation.[24] The micelle dissociates after Dap inserts into the bilayer, which is promoted by the lipid tail. It was speculated that Dap oligomerizes inside the membrane to form pores.

Using FRET (fluorescence resonance energy transfer) between the kyn residue of unlabeled Dap and a fully active Dap derivative containing a fluorescently labeled Orn residue, the Palmer group demonstrated that Dap forms oligomers on liposome membranes.[26] Oligomerization occurs under conditions that resemble those required for its antibacterial activity,

suggesting that the oligomer is involved in the bactericidal effect. Moreover, they demonstrated that Dap does not oligomerize in the presence of just Ca^{+2} alone when at physiologically relevant concentrations. The NMR studies performed by Ho *et al.*[25] discussed above were performed with a Dap concentration (2.0 mM) much greater than what is physiologically relevant and so it is possible that micelle formation does not occur in vivo upon Dap binding Ca^{+2}.[26]

Very recently the Taylor and Palmer groups used perylene excimer fluorescence to further characterize Dap oligomerization.[27] The *N*-terminal decanoyl chain was replaced with perylene-butanoic acid. The perylene derivative exhibited an MIC with *Bacillus subtilis* that was 3 times greater than native Dap. On liposomes containing PG, as well as on *Bacillus subtilis* cells, the perylene-labeled Dap formed excimers, which shows that the N-terminal acyl chains of neighboring oligomer subunits are in immediate contact with one another. The extent of oligomerization exceeded 90% on model membranes that contain 50% PG and it is only slightly lower on bacterial membranes. This high extent of oligomerization supports the notion that it is the oligomer that causes the bactericidal effect. In a lipid bicelle system, oligomer formation was titrated with stoichiometric amounts of PG. Therefore, the interaction of Dap with a single molecule of PG is sufficient to trigger Dap oligomerization.

Fluorescence studies performed on *B. subtilis* showed that when Dap binds to the membrane, it alters the morphology of the cell, shown in figure 1.4.[28] Membrane bulges are seen to form at both sub- and supra-MIC concentrations. At sub-MIC concentrations, the outer leaflet bulges are met with bulges on the inner leaflet, most likely caused by localized cardiolipin. This distortion will be recognized by the cell division protein DivIVA, which will identify this as a location of possible cell division. This process does not lead to cell death, however it does lead to a noticeable bend in the rod structure of the cell.[28] At supra-MIC concentrations, multiple sites of

membrane bulging will occur, presumably overwhelming the ability of the cell to compensate through membrane changes, resulting in pore formation in the cell membrane.[28] It appears that Dap forms pores upon oligomerization in the cell membrane as it has been shown that Dap depolarizes the bacterial membrane resulting in escape of intracellular ions, mainly potassium, leading to a loss of membrane potential.[29] This may be the primary cause of cell death. Aside from the leakage of the ions, it has also been shown that leakage of cell wall amino acids, as well as the formation of sugar-peptide precursors and peptidoglycans are disrupted by Dap.[30]

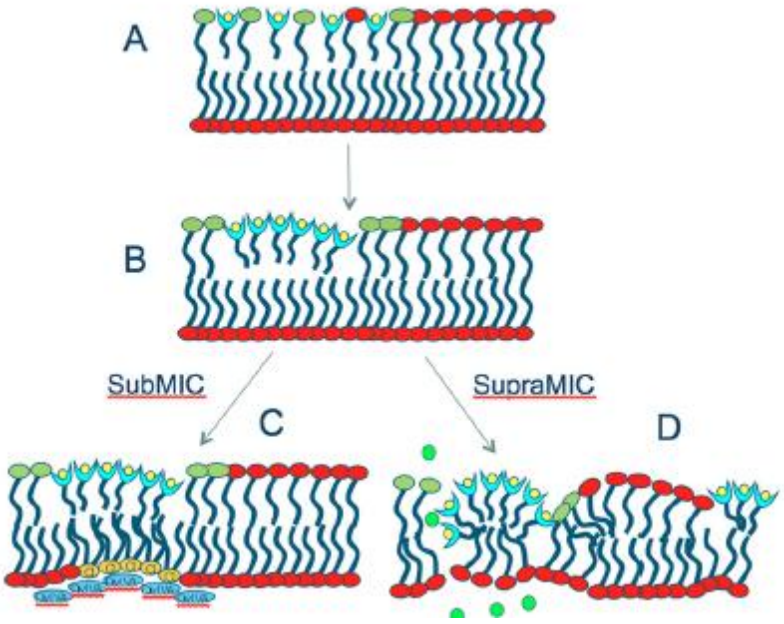

Figure 1.4: A possible mechanism of action model of Dap showing cell morphology being altered at both sub and supra-MIC concentrations. (Dap = blue cups with yellow circles, PG = green lipids, cardiolipin = yellow lipids, K^+ ions = green circles, DivIVA = blue ovals). Taken with permission from reference 28.

1.2.4 Mechanisms of Resistance

Understanding the mechanism of resistance to an antibiotic can often aid in the understanding of the mechanism of action. Clinical cases of nonsusceptibility during Dap therapy have been observed for *E. faecium*,[31] methicillin-resistant *S. epidermidis*, methicilin-resistant

Streptococcus sanguis[32], *E. faecalis*,[33] and MRSA.[34,35,36] This is a cause for some concern as Dap is often used as a last-resort antibiotic for treating certain MRSA and VRSA infections.

A definitive mechanism of resistance to Dap has not yet been identified. However, very recently it has been shown that in vitro development of Dap resistance in *S. aureus* is correlated with the loss of an 81 kDa membrane protein.[37] Moreover, mutations in clinical Dap resistance isolates have been shown to occur in the mprF (multiple peptide resistance factor)[38,39] gene and yycG gene.[38]

The MprF protein catalyzes the coupling of lysine to PG to give LysylPG (LPG). Membranes lacking LPG are more acidic than those containing PG and LPG. Dap resistant strains with mprF mutations have membranes with increased ratios of LPG/PG.[40] Deletion of mprF in S. *aureus* caused increased susceptibility to Dap by about four-fold.[41] It is likely that the increased positive charge imparted by LPG in Dap resistant mutants reduces Dap-lipid interactions due to a less favorable electrostatic interaction.

The YycG protein is a membrane spanning sensor/histidine kinase of a system that partners with the YycF response regulator protein. Upon external stimulus, the YycG protein undergoes an autophosphorylation event at a histidine residue. YycG then catalyzes the transfer of the phosphate group to an aspartic acid residue on YycF (the response regulator). Phosphorylation causes the response regulator's conformation to change, usually activating an attached output domain, which then leads to the stimulation (or repression) of expression of target genes. This is typical of a bacterial signal transduction cascade. In *S. aureus* and many other Gram-positive bacteria, YycFG is the only two-component system required for viability. It functions as a master regulatory system for cell wall metabolism and biofilm formation.[42,43] YycG is localized to the cell division septum in *B. subtilis* where it regulates cell division and wall restructuring.[44] Dap

inserts preferentially into membranes enriched for PG localized at the cell division septum in *B. subtilis*.[45] This causes rapid cell death without lysis and the formation of aberrant cell division septa.[46] Moreover, the yycFG two component regulatory genes are not present in Gram negative bacteria. Dap does not inhibit the growth of Gram-negative bacteria, including an E. *coli imp* mutant defective in outer membrane assembly (MIC of 128 ug/mL).[47] On the other hand, vancomycin, which like Dap does not penetrate the outer membrane of *E. coli*, has an MIC of 0.8 μg/mL against *E. coli imp*.[48] Though it should be stressed that the outer membrane of the cell wall in Gram negative bacteria most likely also plays a role in their resistance to Dap. Nevertheless, it is possible that Dap binds to YycG and blocks signal transduction. Consequently, Baltz has proposed a novel, dual mechanism of action of Dap: inhibition of YycFG-mediated signal transduction and disruption of membrane function.[49]

Vancomycin-resistant enterococci (VRE) is another very important example of a multidrug resistant organism that Dap is used to combat. Reports of Dap-resistant VRE have recently appeared which is a cause for some concern.[31,50]

Studies have recently been done to determine the mechanism of resistance in vancomycin-resistant *E. faecalis* and *E. faecium* recovered from patients both before and after Dap therapy was given. This study revealed mutations in two groups of genes in Dap-resistant *E. faecalis* and *E. faecium*. The first group of genes that were altered, *liaFSR*, encodes a three-component system that is involved in the regulation of cell envelope homeostasis.[51] Munita et al. have shown that the deletion of Ile177 in liaF (lipid II-interacting-antibiotic protein) was sufficient to decrease cell susceptibility to Dap.[52] It has since been found that mutations in the LiaFSR system are commonly observed in Dap resistant strains of *E. faecium*.[53,54] The second group of genes in which mutations were identified in Dap-resistance in *E. faecium* encode for enzymes that catalyze reactions

implicated in the cell membrane phospholipid metabolism: glycerophosphodiester phosphodiesterase (GdpD) and cardiolipin synthase (Cls).[53] This was not unexpected as cell phospholipid composition has long been thought to be important.[55] Others had reported that mutations that enhance cardiolipin synthase (Cls) activity were found in resistant Enterococcus strains.[56,57] A decrease in PG and an increase in negatively charge phospholipid content was observed in Dap-resistant *E. faecalis* and *E. faecium* cells isolated from patients after Dap treatment had been given, suggesting that a more positive surface charge was not the main cause of Dap resistance.[55]

Using boron-dipyrromethane-labelled Dap (BDP-DAP), a study was performed by Tran et al. on Dap-resistant strains of *E. faecalis* to learn more about its mechanism of resistance to Dap.[33] What was discovered is that *E. faecalis* uses a mechanism of resistance that is completely distinct from that of *S. aureus* and *B. subtilis*. The BPD-DAP was not repelled from the surface of the resistant strain of *E. faecalis*, indicating that its mechanism of resistance does not rely on repulsion of cationic calcium-dependent Dap from cell wall envelopes as had previously been proposed.[45,58,59,60] It was also discovered that the amount of Dap that is binding to the cell is very similar between resistant and non-resistant strains of the cells, which suggests that the amount of Dap binding is not critical to resistance.[33]

As mentioned above, mutations in Cls were implicated in conferring resistance to Dap. To determine how cardiolipin (CL) is dispersed in the cell wall structure Tran et al. used a hydrophobic fluorescent dye, 10-N-nonyl-acridine orange (NAO) to stain *E. faecalis* cells.[33] NAO interacts with CL-enriched microdomains in the cell membrane that can be visualized by fluorescence microscopy. Using this NAO staining technique, it had previously been determined in both *E. coli* and *B. subtilis* that the CL rich regions of the cell are localized around the division

septa and cell poles.[61,62,63,64] NAO staining of Dap-susceptible *E. faecalis* showed CL rich areas at the poles and division septum as well, however the Dap resistant strains showed a striking change in CL distribution.[33] The CL in the Dap-resistant strains were redistributed away from the division septa, which strongly suggests that this redistribution is a major cause of Dap being redirected away from the division septa in resistant strains of *E. faecalis*.[33] Deletion of Ile177 in the LiaF protein was enough to cause a change in the distribution of CL without affecting the membrane phospholipid (PL) composition.[33] It was suggested that the LiaFSR system, which was in fact predicted to regulate the cell envelope response to these antimicrobial peptides, causes a redistribution (but no change in content) of PL in the membrane.[33]

While PL redistribution is in fact important, it was not substantial enough to confer clinical resistance. What was needed in order to obtain high levels of resistance was substitutions in GdpD and Cls.[33] Introducing a Cls mutation (single amino acid change at position 61) into a strain of *E. faecalis* harboring mutated liaF and gdpD genes produced a change in PL content and DAP resistance similar to that found in a clinically resistant strains of *E. faecali*.[33] The CLs mutant could be introduced only when the LiaF and GdpD substitutions were also present, suggesting that mutations in Cls that result in altering its activity may be compatible only under specific cell membrane conditions and that changes in CLs activity may be deleterious unless compensatory events also occur.[33]

On the basis of the above studies a mechanism of resistance for *E. faecalis* was suggested.[33] In Dap susceptible cells, CL-rich domains are located at the poles and division septa, allowing calcium-dependent Dap to bind, accumulating at the septum, impairing cell division and resulting in cell death.[33] In Dap resistant *E. faecalis*, an activation of the LiaSR two-component regulatory system causes a redistribution of CL in the membrane away from the cell division septum.

Subsequent changes in GdpD and Cls alters the PL composition and reduces PG content in the cell membrane. Due to these changes, Dap is diverted from the cell division septa to sites in which it cannot oligomerize due to an increased richness in negatively charged PLs.[33] This results in Dap not being able to distort the membrane, which allows enterococci cells to survive Dap treatment.

In the above proposed mechanism it is not clear as to whether the presence of increased CL in membranes results in an increase or decrease in Dap activity. Very recently, the Palmer and Taylor groups in collaboration with others have shown that when CL is added at molar fractions of 10% or 20% to model membranes containing PG, daptomycin no longer forms pores or translocates to the inner membrane leaflet. Dap continues to form oligomers; however, these oligomers contain only close to four subunits, which is approximately half as many as observed on membranes without CL.[65] They proposed that a Dap pore consists of two aligned tetramers in opposite leaflets, and that CL prevents the translocation of tetramers to the inner leaflet, thereby forestalling the formation of complete, functional octameric pores.[65]

1.3 Photoaffinity Labeling

1.3.1 Background of Photoaffinity Labeling

Some of the studies on Dap resistance discussed above suggest that Dap may be interacting not only with specific lipids in the cell membrane but also specific proteins. Determining whether or not Dap interacts with specific proteins (and lipids) is important as it would shed light on its mechanism of action and resistance mechanisms.

Photoaffinity labelling (PAL) is a method that can provide insight into interactions between a ligand and its target or in this case, interactions between Dap and proteins and possibly lipids. PAL was developed over five decades ago by Westheimer,[66] and has remained largely unchanged.

With PAL, a photoactive group is appended to a ligand (figure 1.5).[67] This group does not significantly reduce the activity of the ligand in comparison to the non-derivatized form. The ligand-photo probe (photoaffinity label) is introduced into a biological system and a complex is formed between the photoaffinity label and its biological target. The system is irradiated to trigger the photoactive group on the molecule and produce a reactive species such as a nitrene or carbene.[67] The reactive species forms a covalent bond between the photoaffinity label and the biological target.[67] The ligand and its covalently bound target are isolated. If the ligand is bound to a protein, the covalent complex is subjected to proteolytic digestion and the resulting peptides are sequenced to identify the target.

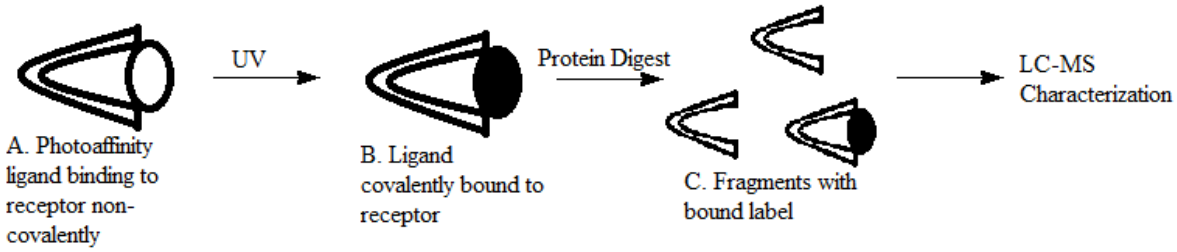

Figure 1.5: General process for PAL.[67]

1.3.2 Photoaffinty Probes

Typically, photoaffinity probes (PAP) contain three functionalities, a pharmacore (the target ligand), a photoreactive group, and a tag for finding the bound groups.[68] Ideally, a PAP should have the following attributes: it will need to be stable in the dark, or even ambient light; it should remain similar to the target molecule, with little change in activity; remain sterically unhindered; have an activation wavelength that does not damage the other components of the system, such as the target proteins; a highly reactive photo-intermediate with a short lifetime will need to be generated upon radiation; it will need to be able to react with any type of bond or residue

without preference; and it will need to form a stable adduct with the target protein or enzyme in order to survive the workup and isolation.[69,70] There have been no reported probes to date with all of the above characteristics.

The three most commonly used photoreactive groups that are implemented into PAPs consist of benzophenones (**1.1**), arylazides (**1.2**), and diazirines (**1.3**), which are all depicted below in figure 1.6. These groups are all discussed in detail in the following sections.

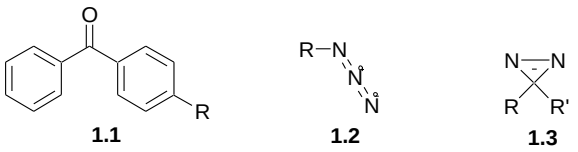

Figure 1.6: Commonly used photoreactive groups: (a) benzophenone, (b) aryl azide and (c) diazirine.[68]

1.3.2.1 Benzophenones as a Photoaffinity Labels

Benzophenones (BP) and other aryl ketone photophores are usually the photoactive group of choice when performing a high efficiency covalent modification of a target.[71-74] Benzophenone is the most used aryl ketone, due to the fact that it has triplet-state properties which are needed for most biochemical studies.[71] BPs do however have some drawbacks, such as the fact that its size and hydrophobicity can make interaction with relatively small ligands a problem, and can potentially lead to non-specific labelling.[71] Below in figure 1.7, the basic steps of radical photolabelling are shown, including the triplet state excitation, H-abstraction, and radical recombination when creating the covalent link between the photolabel and the target.

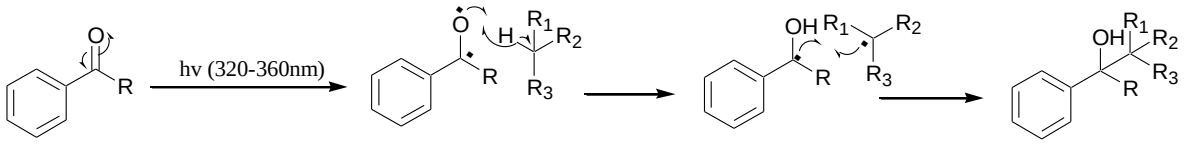

Figure 1.7: Formation of covalent adducts from photoexcited BP (R=benzene).[75,76]

Benzophenones are known to have many advantages over other carbene and nitrene based photoaffinity labels, which makes them particularly attractive in biochemical studies. BPs are chemically stable to many acids and bases when compared to most other photoaffinity labels.[71] They are stable in ambient light, meaning that they can be manipulated without significant degradations.[75] They are activated by UV light between 330 and 360nm which is less damaging to the target proteins as the activation wavelength is sufficiently high enough to avoid protein denaturation.[75] The BPs are also still very reactive with C-H bonds even in the presence of water.[75] The activation of a benzophenone is not photodissociative, and the reaction by C-H insertion is dominant with benzophenones, resulting in stable covalent adducts that can survive chemical and enzymatic peptide cleavage.[71]

The behavior of the n,π^* triplet state of aryl ketones is similar to that of alkoxy radicals in a bimolecular reaction which leads to the abstraction of a hydrogen atom, while the π,π^* state shows low bimolecular reactivity.[77] From this it can be deduced that for photolabelling studies, the n,π^* state is wanted in order to have efficient photophore attachment to the target molecule. In simple BPs, the n-π^* near UV absorption at 330-360nm is usually weak, but well separated from the π-π^* transition.[71] Also worth noting is that when substituted, BPs usually keep their pre dominant n-π^* energy transition.

Benzophenone photophores generally abstract hydrogens from sterically accessible C-H bonds of amino acids and other substrates generally consistent with the C-H bond dissociation

energies.[75,78] A study had been done to correlate bond breaking energies with the possible H-abstraction and crosslinking sites.[79] Tyrosine has two energetically equivalent H-abstraction points, the phenolic and the benzylic sites.[79] Like tyrosine, cysteine is a very good H-donor for the excited benzophenones, however the recombining thioacetal is not stable enough to allow for isolation and characterization. Instead what is frequently isolated is methionine as a crosslinked site due to the stabilization caused by the adjacent heteroatoms.[79]

The lifetime of the photoexcited state of benzophenone varies depending on concentration, pH, solvent as well as the other interactions that could be happening in solution.[79] In organized media (eg. cyclodextrin complexes) the lifetime is much shorter (10-100 ns) than in a glucose monomer solution.[80] The reactive distance for the abstraction of a hydrogen is 2.5-3.1 Å.[75] Because of this, depending on the binding affinity of the compound, even shorter triplet states than mentioned above would efficiently abstract a hydrogen atom from a bound site.[71] H-abstractions typically tend to be highly regioselective, which is very important due to the fact that virtually all photoaffinity labelling studies are designed for interaction with a specific macromolecule, in which selectivity and efficiency would be desired.[71]

The site selectivity of the benzophenone photophores is very useful in ligand-protein interactions. A single attachment point with a protein yields valuable information about the arrangement of amino acids in the binding site in three dimensions.[71] Other highly reactive photolabels, such as diazarenes and azido comopounds, often label several amino acids in the binding domain, often preferring nucleophilic residues rather than the residues that are in close proximity.[79] This, while sometimes useful, mostly results in an unnecessary complication of analysis of specifically labelled peptide fragments, particularly when the efficiency of the labelling is low.[71]

When looking to design a BP photoaffinity label, nonspecific labelling can be reduced if the BP is integrated as part of the macrophore, these are referred to as "endo" photolabels.[71] To design a photolabel such as this, the BP would be used to replace a hydrophobic portion of the molecules. For example, the BP can be attached to macromolecule through diaryl ethers, thioethers as well as amines without losing a significant amount of activity.[81,82] Another type of benzophenone photolabel is referred to as an "exo" photolabel, which is often also called a "tethered photophores".[71] A tethered photophore is attached to the macromolecule via a flexible linker, and often positions some distance from the ligand recognition site.[71] This method, through optimization of the linker can still result in highly specific photoattachment parameters.[71]

Benzophenones being incorporated into peptides has given many useful photoprobes for studying the peptide-protein interactions. These probes have given the ability to identify specific receptor proteins in whole cells or crude protein preparations.[71] BPs have allowed the characterization of pharmacological properties and functional behavior of recombinant or native receptors.[71] BPs have also allowed the ability to map active sites of peptide domains that take part in peptide recognition.[71]

1.3.2.2 Diazirines as Photoaffinity Labels

Diazirines are a very commonly used type of photoaffinity label. They are the smallest type of PAPs. Size of the PAP is important to consider since one wants to avoid significantly altering the size and structure of the ligand since modification of the ligand can alter its activity. In other words, one usually wants as small a photophore as possible. One advantage of diazirines over azides is that several studies have shown that diazirines are more stable to light, as well as acidic and alkaline media, than azides in almost every case.[83,84]

When irradiated at a wavelength of 355 nm, diazirines generate a highly reactive carbene, which is a molecule containing a neutral carbon atom with a valence of two and two unshared (non-bonded) valence electrons (figure 1.8). The non-bonded electrons can be spin-paired and occupy the same non-bonding orbital (called a singlet carbene) or the non-bonding electrons can be unpaired (parallel spins) and occupy separate non-bonding orbitals (called a triplet carbene).[85] The singlet state is stabilized by electron donating substituents, which will donate electrons to the empty p-orbital.[86] For example, aliphatic diazarenes will isomerize to a diazomethane when irradiated, and thus will create a singlet state carbene.[87] Phenyl diazirine (**1.4**, figure 1.9) and phenylchlorodiazirine **(1.5**, figure 1.9) will produce the singlet phenylcarbene,[88] while p-nitrophenylchlorodiazirine (**1.6**, figure 1.9) and trifluorophenyldiazirine (**1.7**, figure 1.9) will produce a triplet phenylcarbene due to the presence of electron withdrawing groups.[89,90,91]

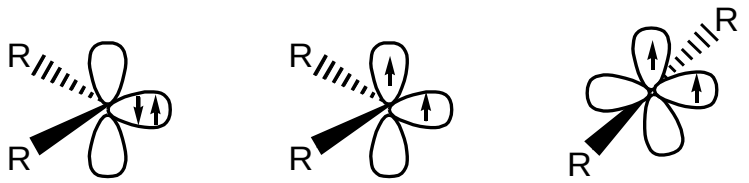

Singlet Triplet sp^2 hybrid Triplet *sp* hybrid

Figure 1.8: Representation of the electronic states of the carbenes.[66]

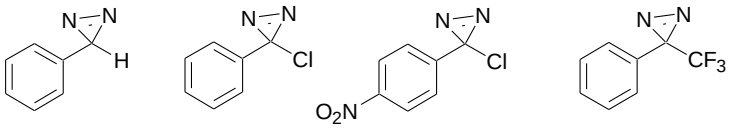

1.4 **1.5** **1.6** **1.7**

Figure 1.9: Aryldiazirines 1.4-1.7.[66]

The single best attribute of a carbene for PAL is its ability to form a covalent bond very rapidly with the nearest target molecule, through C-C, C-H, O-H and H-X (X=heteroatom)

insertions.[66] To go along with their small size, diazirines are very stable at room temperature, are relatively stable around nucleophiles, and are stable in both acidic and alkaline media.[84] Diazirines also have an activation wavelength of 350-355nm, which is long compared to most PAPs, which will reduce damage on biological systems, reducing the risk of harming any proteins or enzymes that are trying to be recovered.[84]

When using a diazirine as a PAL, low yields are commonly seen. This is due to the fact that the carbenes are quickly quenched by water molecules.[66] This feature can sometimes be more of an advantage than a disadvantage as it will minimize the chances of nonspecific labelling, resulting in only ligand molecules that are tightly bound with the receptor reacting to form a covalent bond with the desired protein.[66] The unbound ligands will react with water before undergoing non-specific binding with other proteins.

Despite having all of these advantages however, there are a fair amount of reported failures of diazirine based photoaffinity labelling where other photophores have proved successful.

1.3.2.3 Azides as Photoaffinity Labels

Another common type of photoaffinity labels are aryl azides. In fact, until recently, aryl azides were perhaps the most commonly used photoprobes. Their popularity was mainly due to the fact that they are relatively small in size, they are easily synthesized, they are stable in storage, and they lack reactivity in physiological conditions, so long as there is an absence of light.[92]

Aryl azides are precursors to aryl nitrenes, the nitrogen analogs of carbenes, which are produced when the aryl azide is irradiated with UV light, between 254 and 265nm.[92] There are three major routes of formation of covalent bonds between the aforementioned aryl nitrene and the proteins of interest when using photaffinity labelling, which are illustrated in figure 1.10. The first,

and most obvious of the possible covalent bond formations is a C-H or N-H bond insertion by the nitrene to give a secondary aryl amine, or an aryl hydrazine respectively.[93] Another major product of nitrenes reacting in a membrane is the formation of aziridines, which are produced by the insertion of the nitrene into a double bond of an unsaturated fatty acid.[93] The last major reaction that can take place with a nitrene in the membrane occurs in two steps. First, the ring can expand to form a dehydroazapine intermediate. This intermediate will then react with any N-H or C-H bond nearby to give a variety of azapines.[93] The above reactions are known as productive reactions as they result in the formation of a covalent bond between the photoprobe and biological target.

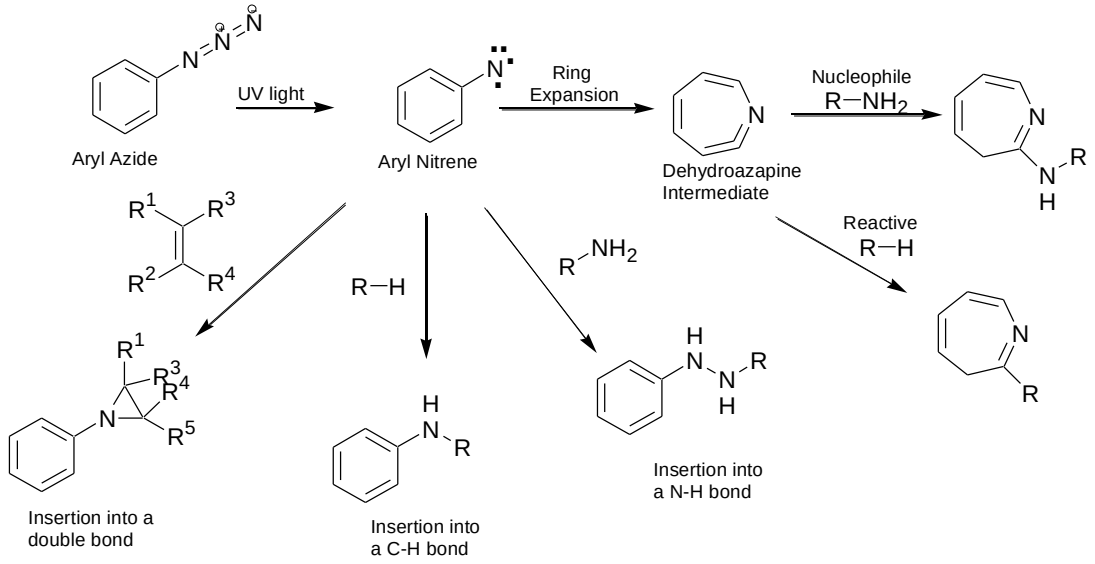

Figure 1.10: Productive reaction pathways of aryl nitrenes[92]

Aside from the productive reactions discussed above, there are a number of non-productive side reactions that commonly take place when using aryl nitrenes, which are illustrated below in figure 1.11. The most common non-productive side reaction that is known to occur in the membrane is a pair of hydrogen extractions, which will leave an unreactive primary aryl amine.[93] Another side reaction known to happen is the dimerization of the aryl nitrenes to produce

azobenzenes.[93] The last currently discovered non-productive side reaction that can happen in these experiments is the non-photochemical reduction of the aryl azide to an aryl amine, which is usually cause by the presence of thiols in the cell structure.[94,95] There are a number of remaining non-productive side reactions of course that happen with the majority of photoaffinity probes, not only the aryl azide based probes. These side reactions can be the cause of non-productive products formed in any of the reactions outlined in figure 1.11. The majority of photoaffinity probes will react with water, buffer molecules, or with components of the cell other than the target structure due to unspecific reactions.[92]

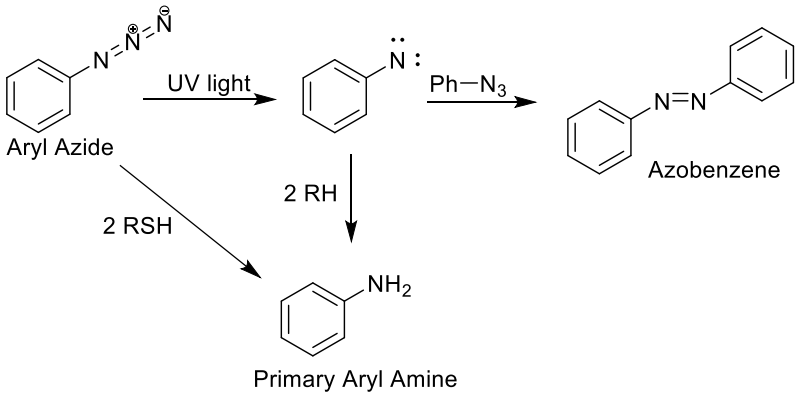

Figure 1.11. Non-productive products of aryl azide photoaffinity probes[92]

The final property of aryl azides that makes them appealing as photoaffinity probes is the fact that their corresponding nitrenes have very short lifetimes in solution. These aryl nitrenes have been estimated to have a lifetime of only 0.1-1ms in model systems.[96] Short lifetimes are very useful when dealing with photoaffinity labelling. This is due to the fact that a short reactive lifetime, in comparison to the rate of dissociation of the label-binding site complex, will result in less chance of non-specific binding.[97,98]

1.3.3 Unraveling the Protein Targets of Vancomycin in Living Cells Using PAL

An excellent example of using a PAP to identify proteins that interact with an antibiotic was recently reported by J. Eirich *et al.*[99] In their study they identified proteins that interact with vancomycin in live cells.

During this study, there were many obstacles to pre-plan in order to successfully complete their objective. The first issue to deal with was determining what type of photoprobe would be most suitable. They chose to use a benzophenone photoprobe since, as mentioned in section 1.3.2.1, benzophenones have the most desirable properties for PAL. However, the concern was that benzophenone, since it is quite large, would significantly affect the biological activity of the antibiotic. Therefore, they prepared three different PAPs in the hope that at least one would be biologically active (probes 1-3 in figure 1.12). Each one contained a benzophenone group as well as an alkyne appendage. The alkyne moiety was included to facilitate the isolation of any vancomycin-protein adducts obtained after the labelling experiment (this will be discussed in more detail below).[100-103] Fortunately, the MIC's of all three probes against *S. aureus*, MRSA, VSE and VRE were similar to vancomycin.[99] An evaluation of the photoaffinity properties of the probes was done which involved testing probe concentration and time of irradiation with VRE and MRSA.[99] Irradiation for 1 hour with 1 μM of the photoprobes was found to provide efficient labelling.

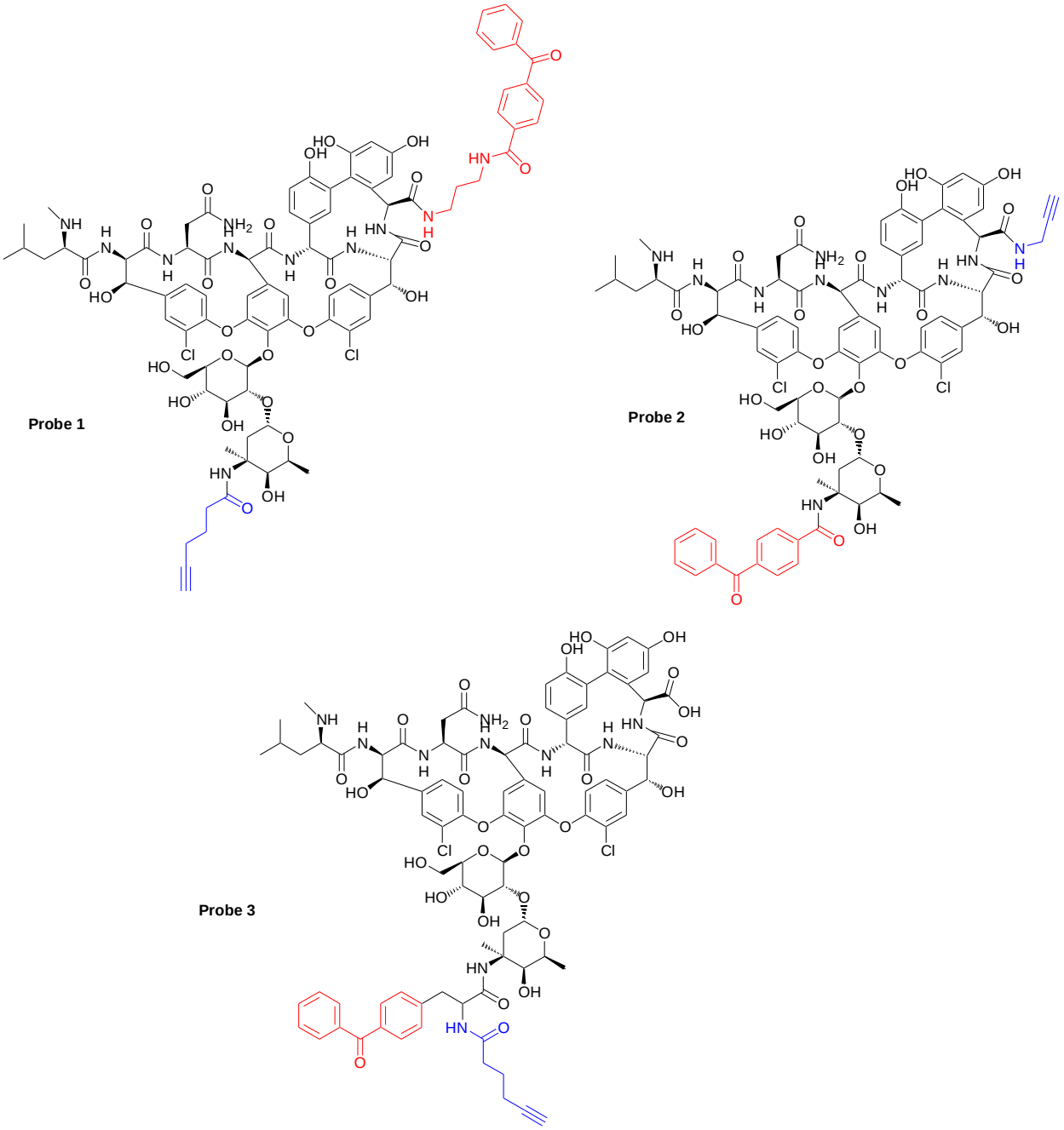

Figure 1.12: The benzophenone photoaffinity probes as designed by J. Eirich *et al.*, showing the photolinker (red) and the benign alkyne tag (blue).[99]

After irradiation, the bacteria were washed and then lysed and the mixture subjected to a commercially available rhodamine-biotin-azide probe and $CuSO_4$. A Huisgen/Sharpless/Meldal reaction (click chemistry) took place between the azido group and the alkyne which resulted in a covalent bond between the rhodamine-biotin probe and the vancomycin-photolabel-protein adducts.[99] After the click chemistry reaction adducts were isolated by applying the mixture to streptavidin-agarose beads. The proteins were released from the beads and then subjected to preparative SDS-PAGE. The fluorescent gel bands were isolated and tryptically digested. The proteins were identified using LC-MS. This study revealed that the proteins that vancomycin interacts with were the bifunctional autolysin in the case of MRSA, and the peptide ABC transporter for VSE.[99]

1.4 Thesis Objective

The objective of this thesis was to design and synthesize a photoaffinity probe for daptomycin. It was anticipated that such a photoaffinity probe will prove to be useful in identifying proteins and possibly lipids that interact with Dap.

Chapter 2 - Synthesis of a Daptomycin Photoaffinity Probe

2 Introduction

2.1 Chemical Modification of Dap

To prepare a Dap photoaffinity probe (Dap-PAP), it was necessary to append a photoactive group to Dap in such a way that there was little or no loss of activity. Dap has been chemically modified extensively, and modifications of the antibiotic are still being performed in attempts to create a structure activity relationship (SAR), as well as to elucidate mechanism of action in more detail. There have been three main areas of modification to Dap; the kynurenine residue, the ornithine residue, and the fatty acyl tail. For our purposes, modification of the tail was not an option as we expected that such a modification would significantly alter Dap's activity. This left the Kyn and Orn residues as points of attachment for the photo probe.

There are two major ways in which the ornithine group has been modified. One approach has been to *N*-acylate the Orn residue using activated esters, anhydrides or guanidylating agents.[3] What was found to be important was that the basicity of the ornithine had to be maintained or, if lost by acylation, another basic NH_2 group had to introduced in reasonably close proximity to the ornithine nitrogen in order to retain good activity.[3] Activity was also shown to decline as *extra* amino groups were added, or as the amino group moved further from the ornithine nitrogen.[3] Aside from this finding, it was also found that coupling long alkyl chains or acidic groups to the ornithine residue led to a large reduction in antibacterial activity.[3]

The second approach to Orn modification is by reductive amination.[104] This method retained the basicity of the ornithine nitrogen which was noted earlier to be important for retaining antibacterial activity.[3] Some of these compounds, in particular ones derived from substituted benzyaldehydes had promising *in vitro* activity; however, on *in vivo* evaluation, it was found that they had higher PD_{50} values than Dap, which is hypothesized to be from an increase in serum protein binding.[3] It was found, however, that some of these compounds exhibited antibacterial activity in vitro, albeit less than Dap, even when the large acyl tail on the tryptophan residue was removed suggesting that the ornithine residue is a secondary site of interaction with bacterial membranes.[3] It is possible that a basic amino group is necessary for Dap-lipid interactions by forming a salt bridge with a phosphate group of PG.

Another area of extensive modification has been the kynurenine (Kyn) residue. This was achieved by diazotizing the amino group on Kyn and then reacting it with a nucleophile (Cl, Br, I, OH, N_3 etc.).[105] However, these modifications usually resulted in a significant decrease in biological activity demonstrating that the free amino group on the Kyn residue is very important to activity.[105]

2.2 Design of the Dap Photoaffinity Probe

Based upon the above discussion, the most logical choice of where to attach the photoactive group was on the ornithine residue. The ornithine residue is not only the easiest point of modification, but a general trend has been noticed that as long as the basicity of the ornithine amino group is kept intact, the activity is not severely affected.[3] The general structure of our proposed Dap-PAP (compound **2.1**) is shown in figure 2.1. We decided to use a benzophenone probe due to its advantages over other photoactive groups that were described in Chapter 1, such good

stability to acids, bases and ambient light, an activation wavelength between 330 and 360 nm, which results in minimal cell damage, and its ability to react with C-H and N-H bonds even in the presence of water.[75] The benzophenone unit would be attached to the Orn residue by an amide or amine linkage. We also appended an alkyne tail to the benzophenone unit which can undergo click chemistry with a tri-functionalized rhodamine-biotin-azide tag for isolation of covalently bound proteins or lipids as described for the vancomycin PAL discussed in Chapter 1. We have chosen to combine the two moieties into one molecule, not only because it will be much easier to attach to Dap, but also because there does not appear to be any other functional groups on Dap that can be modified without significantly altering its activity.

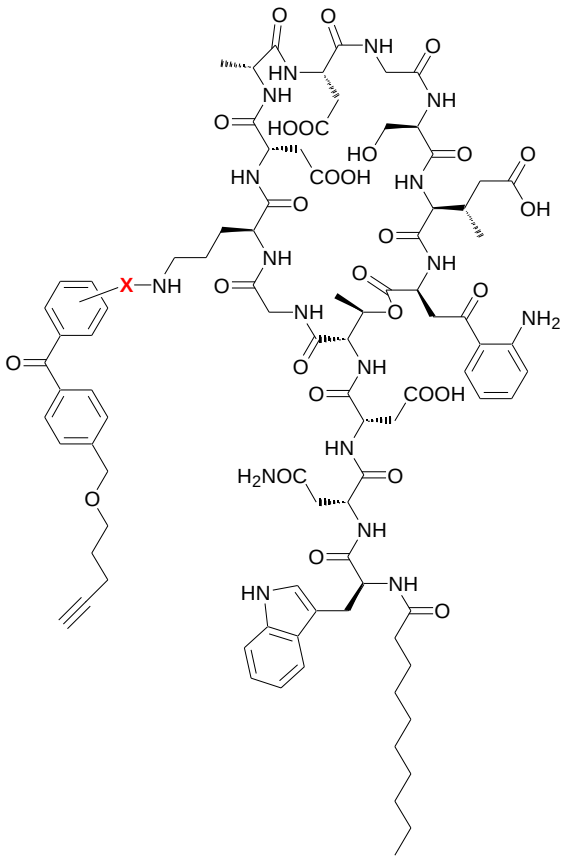

2.1 (X = CH_2 or C=O)

Figure 2.1. General structure of the proposed Dap photoaffinity probe.

2.3 Results and Discussion

2.3.1 An Amide versus an Amine Linkage

There were two ways by which we could attach the benzophenone unit to the Orn residue. One was by an amide linkage and the other by an amine linkage. Based upon the above discussion in section 2.1 an amine linkage would seem to be more suitable as this would maintain the basicity of the amino group which was supposed to be important for activity. However, we anticipated that the synthesis of the PAL containing the amine linkage might turn out to be more challenging than the one containing the amide linkage. Therefore, before embarking upon a synthesis of either compound we decided to prepare Dap analogs **2.2** and **2.3** (figure 2.2) to determine what the difference is in activity when the Orn residue has been acylated as opposed to alkylated. Analog **2.2** has a *p*-trifluoromethylphenyl group attached to the Orn residue by an amide linkage and analog **2.3** has a *p*-trifluoromethylphenyl group attached to the Orn residue by an amine linkage. We chose to append a *p*-trifluoromethylphenyl group to the Orn residue as the reagents that were required to do this were readily available and compounds **2.2** and **2.3** could be used to examine how Dap interacts with membranes using ^{19}F-NMR (these studies would be done by the Dieckmann group in the Dept. of Chemistry at the University of Waterloo).

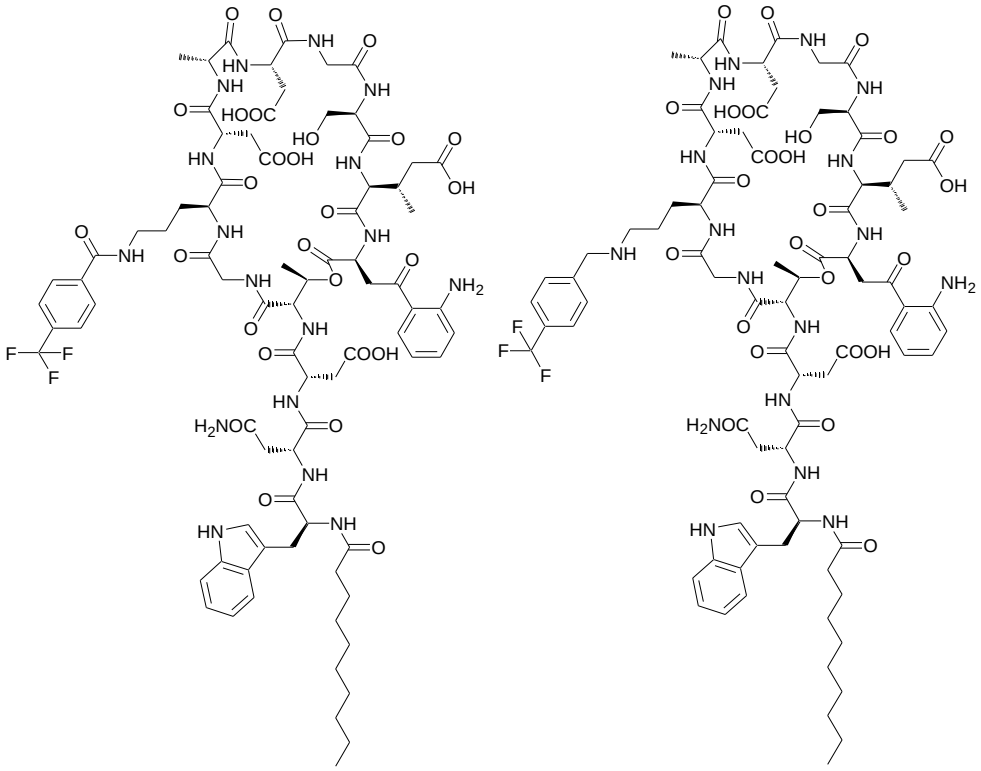

2.2 **2.3**

Figure 2.2. Structures of Dap analogs **2.2** and **2.3**.

In order to create an amide linkage between the 4-trifluoromethylbenzene group and Dap we decided to first activate the acid group in 4-trifluoromethyl benzoic acid using benzotriazole and then react the activated 4-trifluoromethylbenzoic acid (compound **2.4**, scheme 2.1) with Dap as this approach has been used by others to successfully modify the Orn residue of Dap.[3] The synthesis of **2.4** was achieved by adding a 4-trifluoromethylbenzoic acid to a solution of benzotriazole in thionyl chloride at room temperature, and stirring for 4h. After aq. workup and column chromatography compound **2.4** was obtained in a 65% yield.[106]

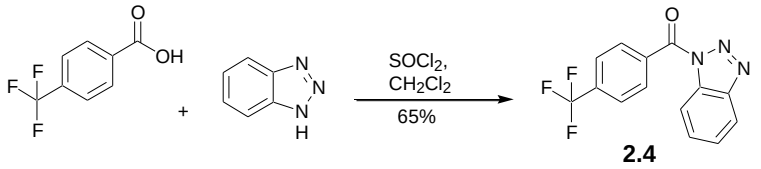

Scheme 2.1. Synthesis of compound **2.4**[106]

To couple **2.4** to Dap, **2.4** was added to a solution of Dap in dry DMF and the reaction was monitored by HPLC until its completion (approximately 24h) (scheme 2.2). Upon completion of the reaction, the mixture was diluted 4-fold with 0.1% TFA in water, and then purified via semi-preparative RP-HPLC (45% yield).[107]

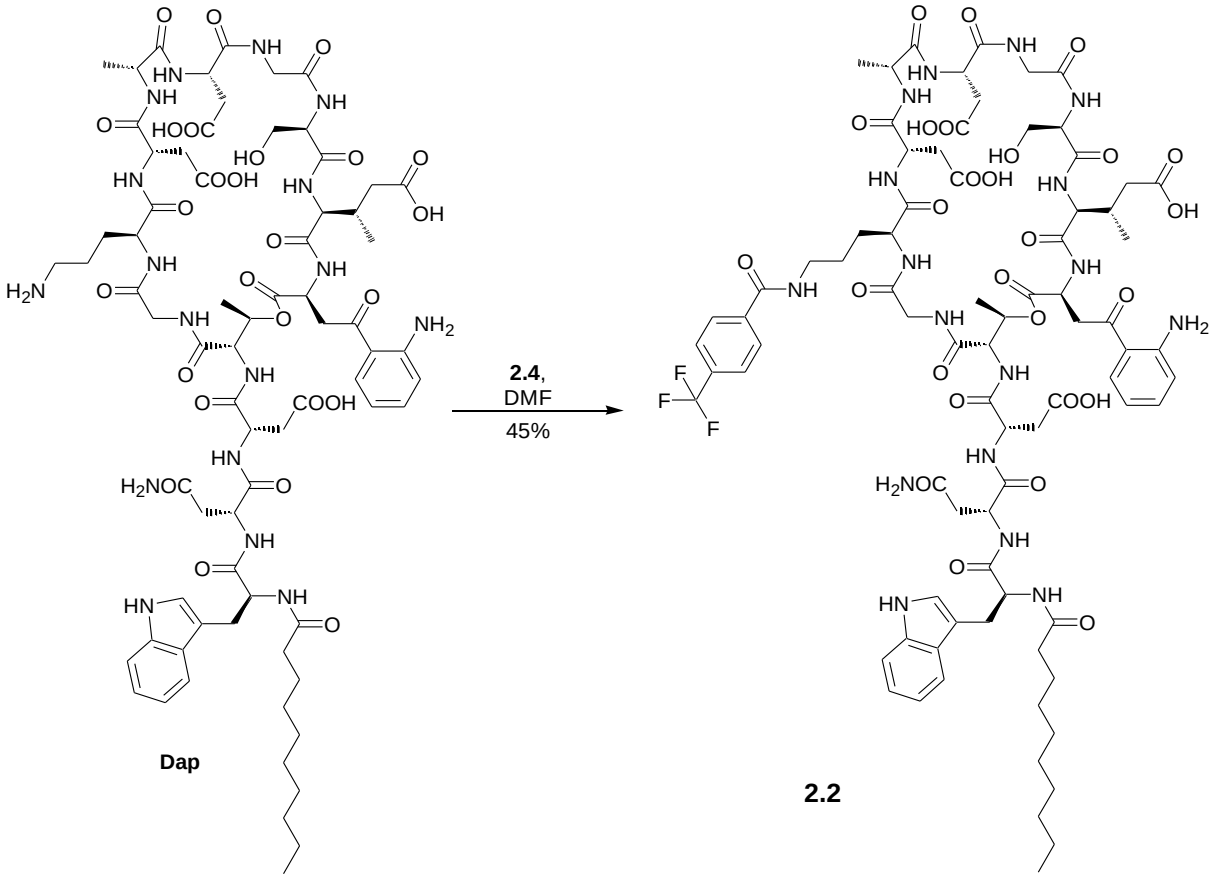

Scheme 2.2. Acylation of Dap with **2.4** to yield Dap analog **2.2**

An analytical RP-HPLC trace of the material after preparative HPLC (figure 2.3) showed 2 peaks: one major peak and one minor peak. We were unable to separate these peaks by semi-preparative HPLC. It is possible that reaction with the Kyn amino group also occurred. The ESI+ mass spectrum (figure 2.4) shows an m/z peak at 896.871 which is the doubly positive charged species. There are no other large mass peaks that could be a result of either starting material, or a doubly modified species of Dap derivative. This supports our hypothesis that the second smaller inseparable peak in the analytical HPLC trace (figure 2.3) is most likely the result of an acylation at the kyn residue, rather than the orn residue. The singly charged species can also be seen on this spectrum in a very small amount at an m/z of approximately 1792.741.

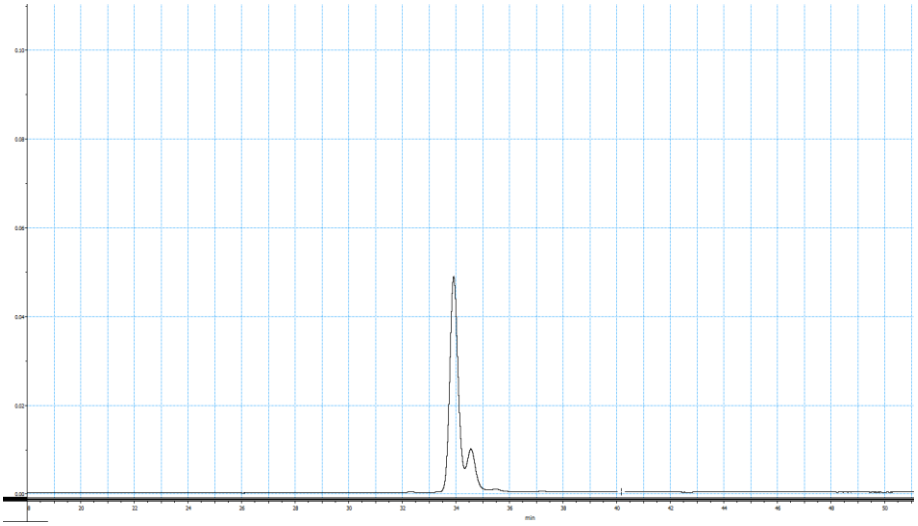

Figure 2.3. Analytical HPLC trace of compound **2.2.**

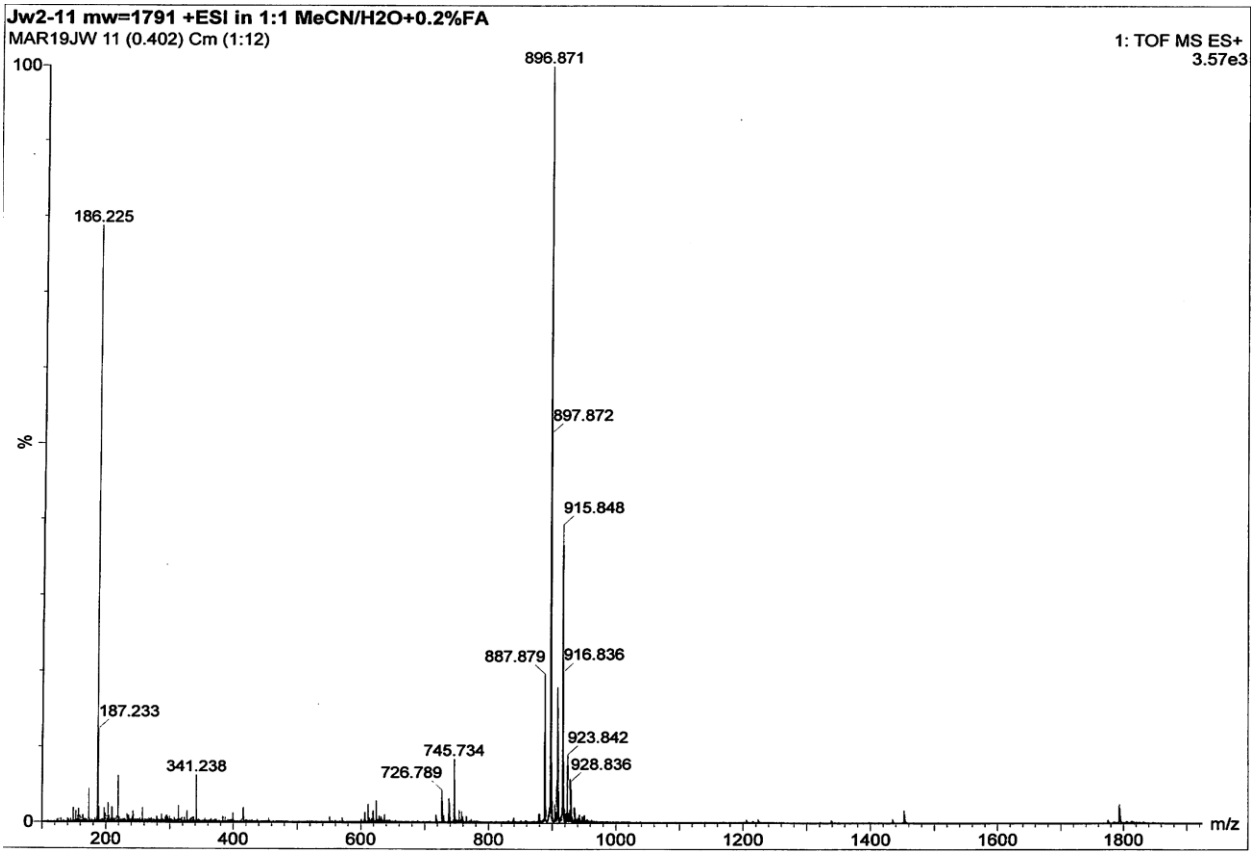

Figure 2.4. ESI^+ mass spectrum of compound **2.2**.

The synthesis of **2.3** was achieved by reductive amination using Dap and 4-trifluoromethylbenzaldehyde (scheme 2.3). To a solution of Dap and 4-trifluoromethylbenzaldehyde in dry DMF was added sodium triacetoxyborohydride (STAB-H) and glacial acetic acid. This reaction was monitored by HPLC until its completion (approximately 24 h). Upon completion of the reaction, it was diluted 4-fold with 0.1% TFA in water, and purified via preparative HPLC (16% yield).[108]

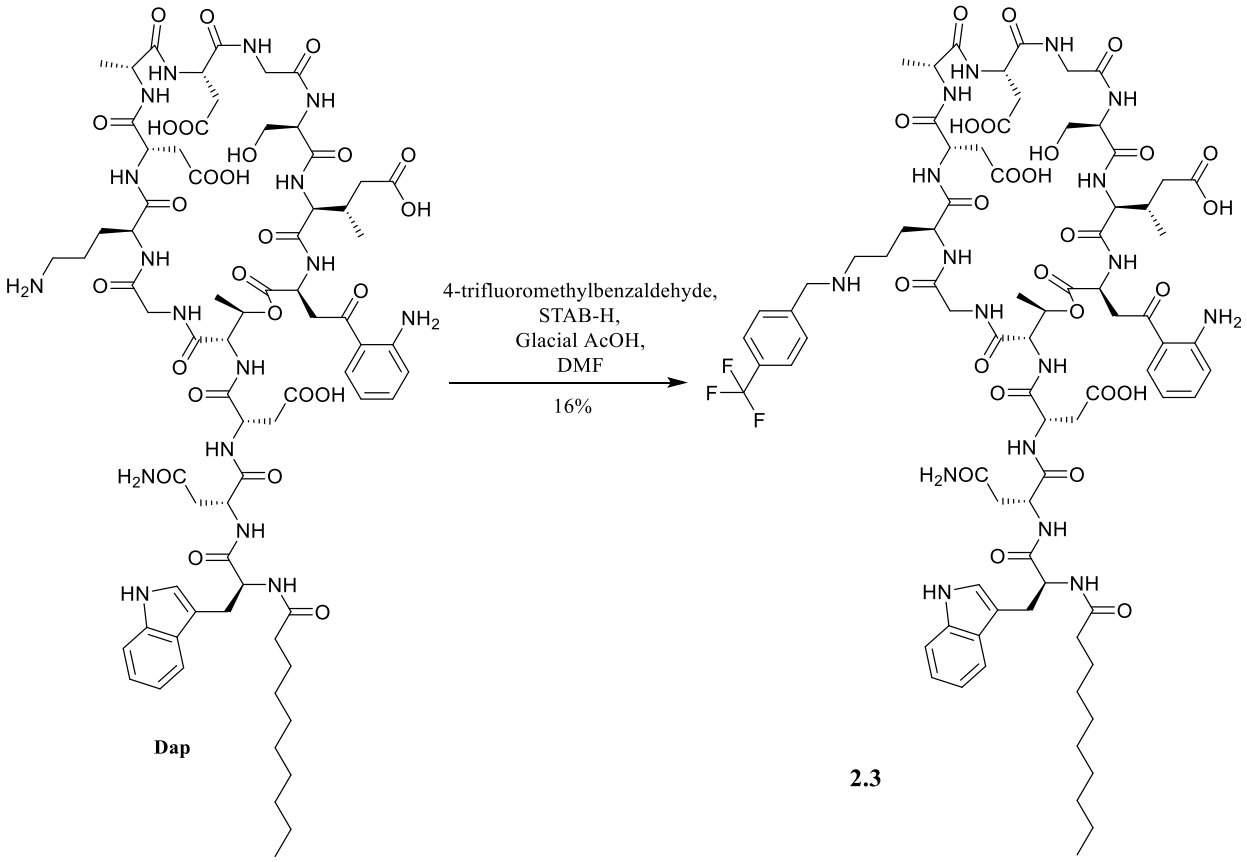

Scheme 2.3. Reductive amination of Dap to yield compound **2.3.**

An analytical HPLC chromatogram of the material after preparative HPLC (figure 2.5) showed one peak confirming its purity. The mass spectrum of this material is shown in figure 2.6. As can be seen, the mass spectrum of compound **2.3** is very clean, showing very little impurity or fragmentation, and also showing a m/z peak at 890.351, once again occurring at this low mass number due to the fact that the Dap species typically are seen doubly positive charged in +ESI mass spectrometry. The singly charged species can also be seen on this spectrum at an m/z of approximately 1778.787.

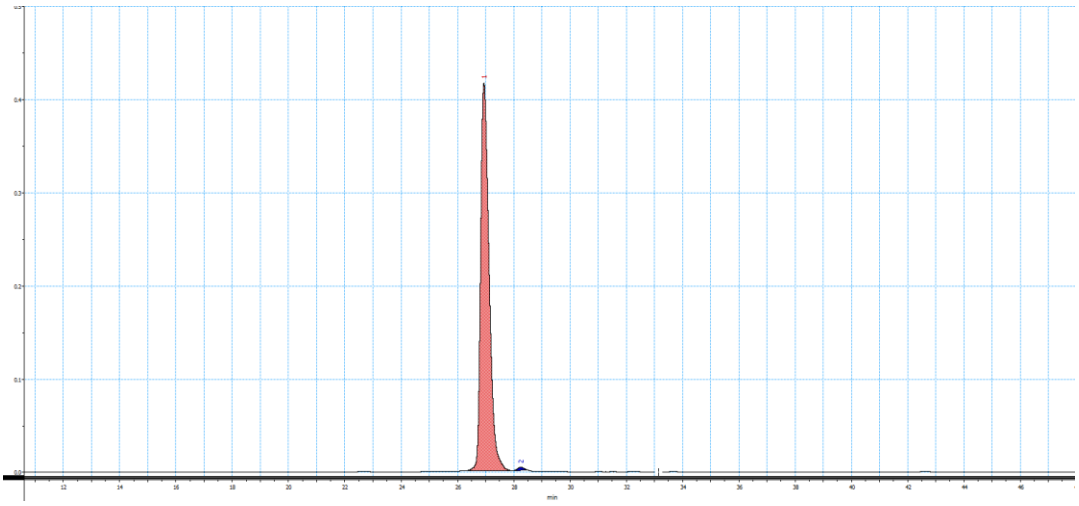

Figure 2.5. Analytical HPLC chromatogram of compound **2.3**.

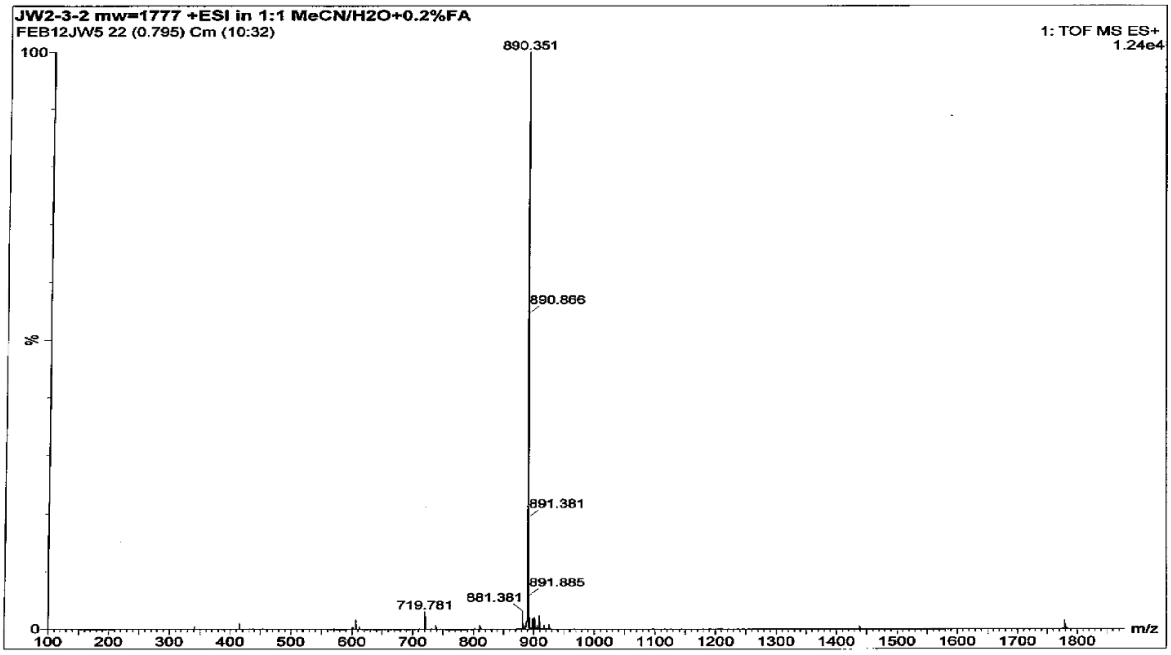

Figure 2.6. ESI^+ mass spectrum of compound **2.2**.

The minimum inhibitory concentrations (MICs) of **2.2** and **2.3** were determined using a lysogeny broth dilution assay as described by Muraih *et al.*[109] Lysogeny broth containing 5 mM

calcium chloride was added to test tubes, to which specific amounts of native DAP or compounds **2.2** or **2.3** were added according to their intended final concentration. Concentrations ranged from 0.25 μg/mL to 10 μg/mL, including a growth control without antibiotic. Each test tube is inoculated with *Bacillus subtilis* ATCC 1046 and incubated at 37 ºC overnight. The following day, growth inhibition was determined by visual observation of turbidity. The results of the test indicated an MIC of native Dap with regards to *B. subtilis* of 0.75 μg/mL, which agrees with the literature value (figure 2.7).[109] The MIC of compounds **2.2** and **2.3** were found to be 3 μg/mL and 2 μg/mL respectively. So compound **2.2** is 50% less active than compound **2.3** indicating that an amine linkage is indeed superiour to an amide linkage though the difference is not as great as expected from the literature studies mentioned in section 2.1.

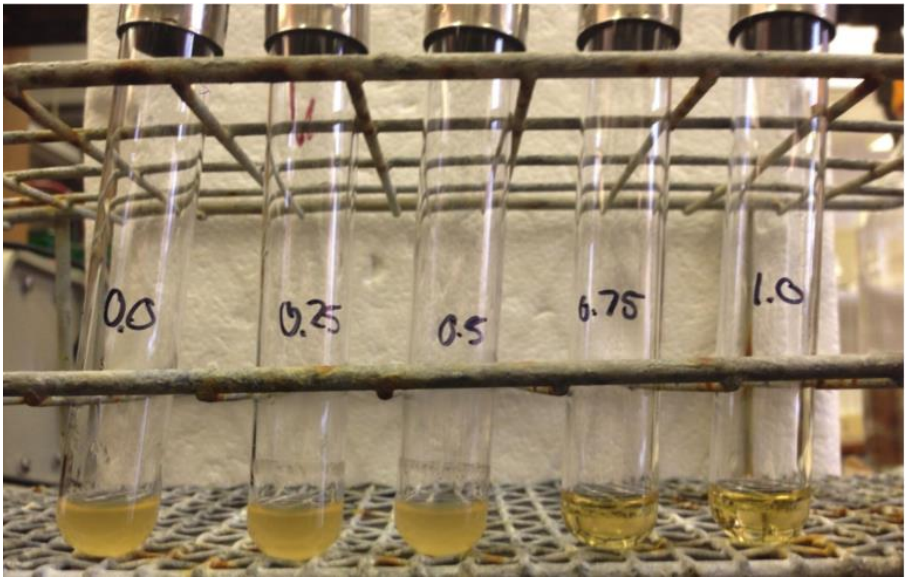

Figure 2.7. Photo of the MIC assay showing concentrations both above (clear) and below (cloudy) the MIC of Dap.

2.3.2 Effect of a Benzophenone Appendage on Dap activity

Before attempting the synthesis of our Dap-PAL we wished to determine if the benzophenone group would significantly alter the antibacterial properties of Dap. Dap analogs **2.5**

and **2.6** were designed to test this and to determine if the point of attachment to the benzophenone group (attaching it via the meta or para position of the benzophenone group) affected activity (figure 2.8).

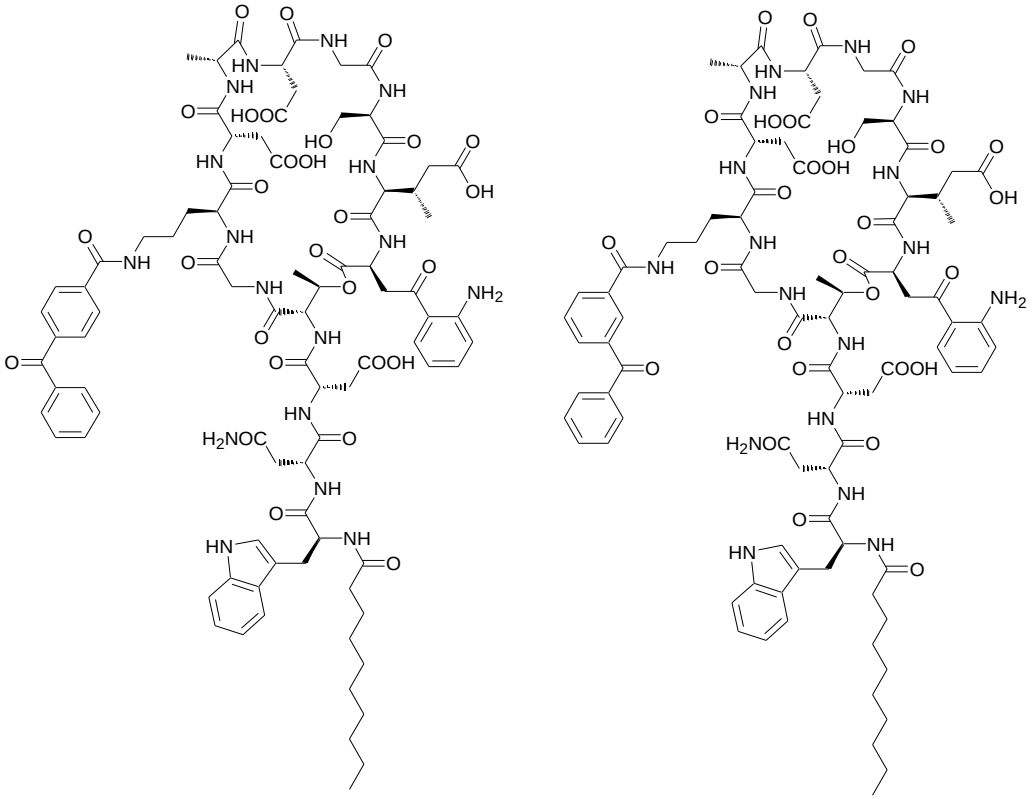

2.5 **2.6**

Figure 2.8. Structures of Dap analogs **2.5** and **2.6**.

The synthesis of compounds **2.5** and **2.6** began with two commercially available compounds, 4-benzoylbenzoic acid, and 3-benzoylbenzoic acid, respectively. These two compounds were converted into their triazole amides (**2.7** and **2.8** in scheme 2.4) using the same procedure as that employed for compound **2.4**.

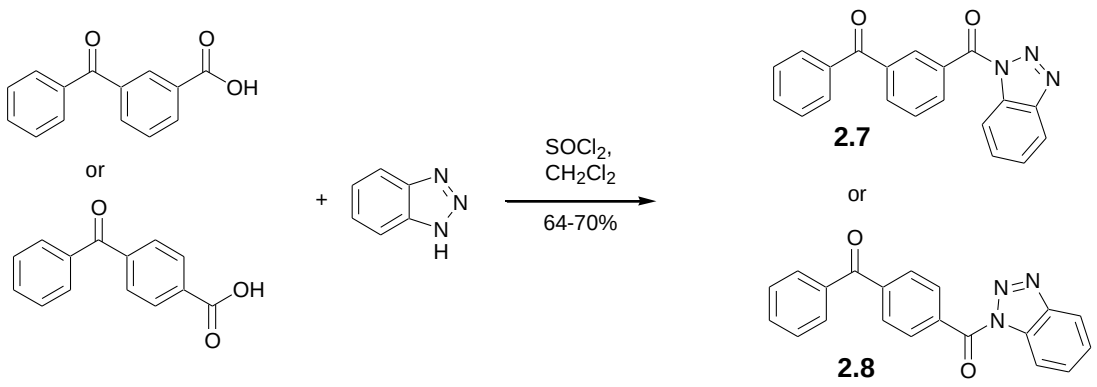

Scheme 2.4. Synthesis of compounds **2.7** and **2.8**[106]

Compounds **2.7** and **2.8** were reacted with Dap in dry DMF for 24 h to give compounds **2.5** and **2.6** in 32 and 35% yields respectively after purification by RP-HLPC (Scheme 2.5).[107]

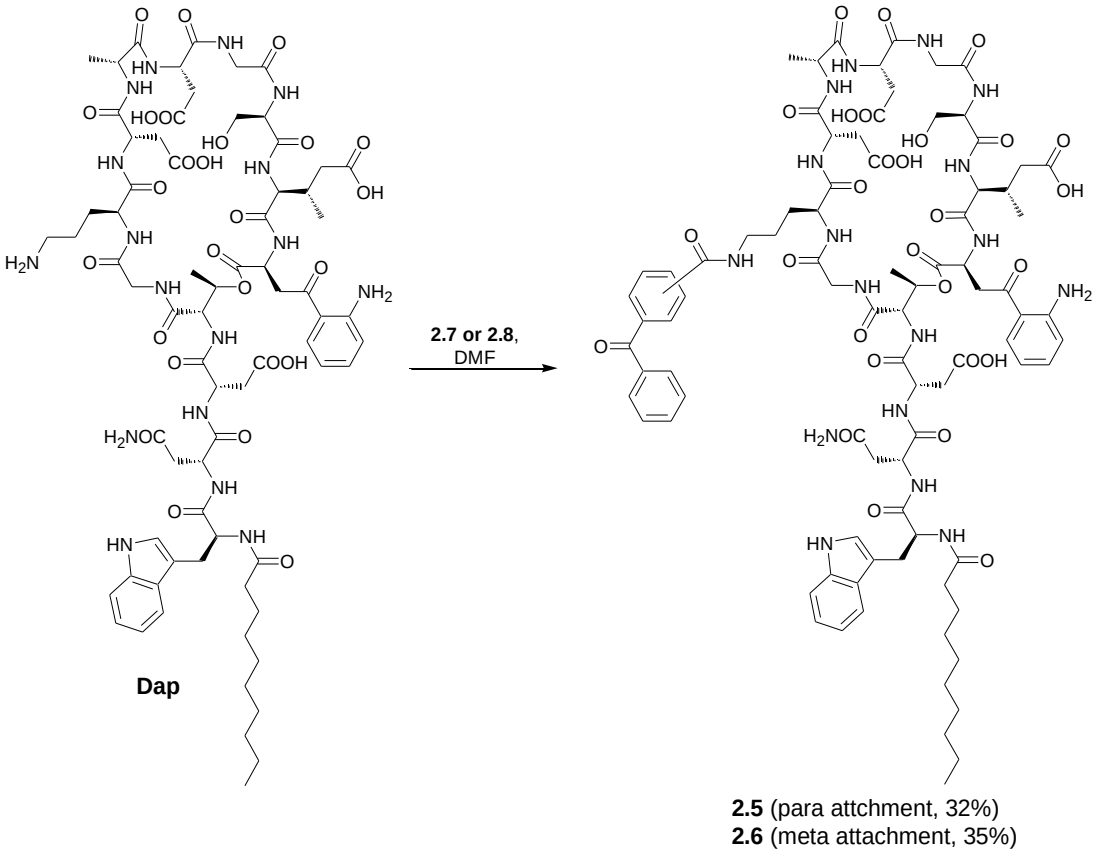

Scheme 2.5. Acylation of Dap to yield compounds **2.5** and **2.6**

The analytical HPLC chromatograms of **2.5** and **2.6** after preparative HPLC are shown in figure 2.9. Each showed one very large peak and a few very minor peaks indicating that sufficient purity was achieved for biological testing. The doubly charged species (m/z peaks at 915.389) of **2.5** and **2.6** are dominant in their +ESI mass spectra (figure 2.10). The singly charged species can also be seen in these spectra at an m/z of 1829.77.

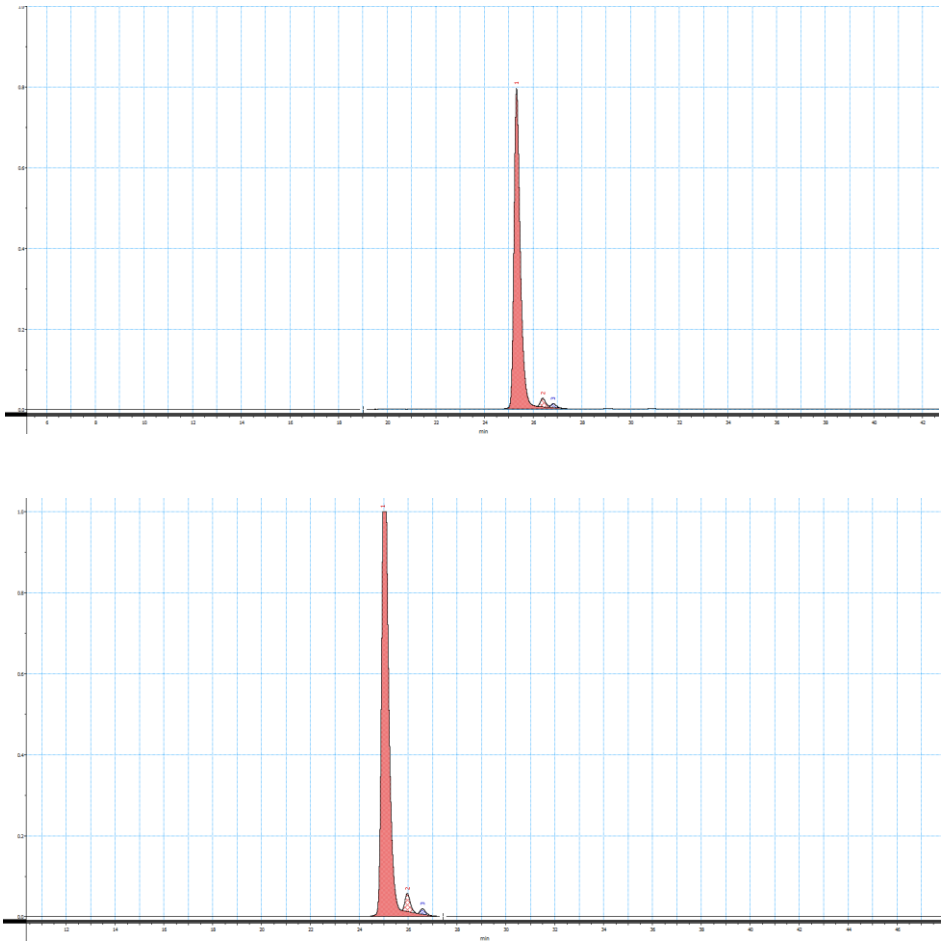

Figure 2.9. Analytical RP-HPLC traces of compounds **2.5** (top) and **2.6** (bottom).

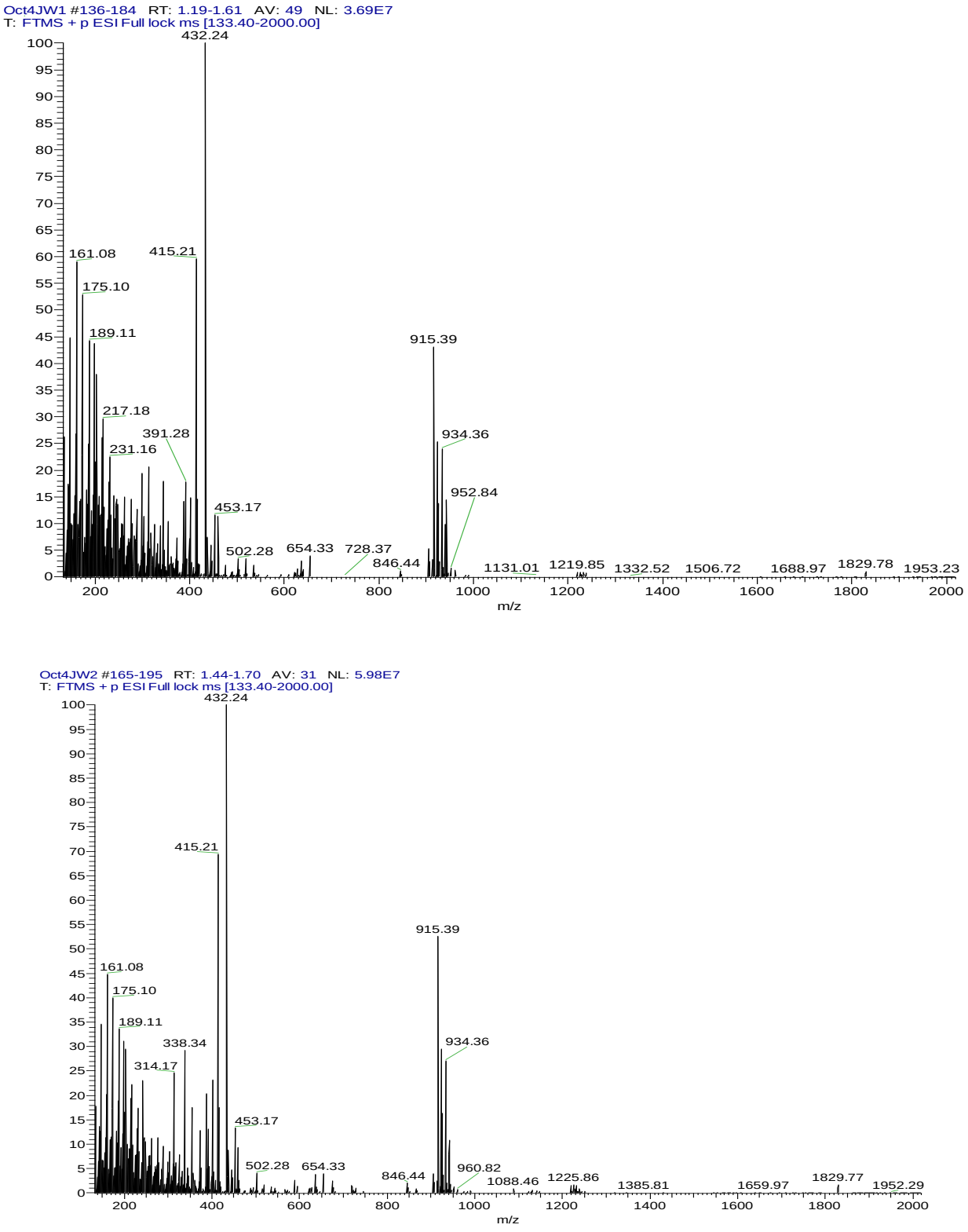

Figure 2.10. ESI^+ mass spectra of compounds **2.5** (top) and **2.6** (bottom).

The MICs of compounds **2.5** and **2.6** were determined using the assay described above and found to be 2 μg/mL and 2.5 μg/mL respectively. This shows that the para linkage may be slightly better than the meta linkage, however it is also quite likely that these two values are within experimental error.

The above results suggested that it would be best to attach the benzophenone photoactive group to Dap via an amine linkage to the para position of the benzophenone group. To attach the benzophenone group to Dap via an amine linkage a reductive amination reaction would have to be performed between a benzoylbenzaldehyde derivative and Dap. One potential complication of this is that the ketone group in the benzoyl benzaldehyde derivative might be reduced during this reaction. To determine if this would be a problem we decided to prepare model Dap derivative **2.9** (figure 2.11).

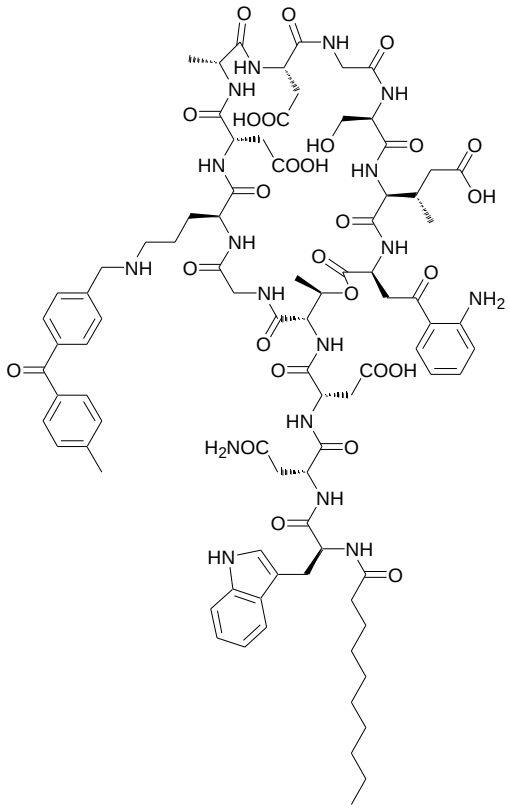

2.9

Figure 2.11. Structure of Dap derivative **2.9**.

The synthesis of compound **2.9** required that we first prepare 4'-methyl-4-benzoylbenzaldehyde (**2.10**). This is a literature compound and has been prepared by a variety of routes. We chose to use the procedure of Gooben *et. al*.[110] To a solution of 4-formylbenzoic acid and *p*-tolylboronic acid in degassed, dry dioxane, under nitrogen in a Schlenk tube was added dimethyl dicarbonate and $Pd(Ph_3)_4$ and the mixture was heated at 80˚C for 18 h. After aq. workup and column chromatography compound **2.10** was obtained in a 40% yield.[110]

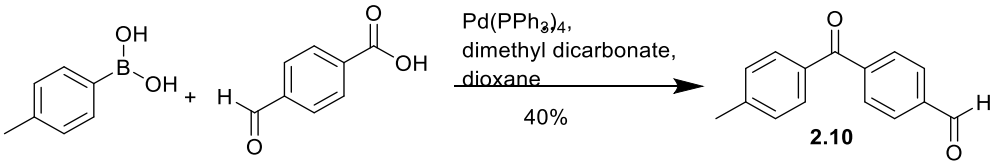

Scheme 2.6. Synthesis of compound **2.10**.[110]

Compound **2.10** was attached to Dap using the reductive amination procedure described above.[108] After purification by semi-preparative RP-HPLC compound **2.9** was obtained in a 23% yield. An analytical HPLC chromatogram of **2.9** after preparative HPLC (figure 2.12) showed one peak confirming its purity. In the ESI+ mass spectrum of **2.9** the doubly positive charged ion was dominant (*m/z* peak at 915.399, figure 2.13). The singly charged species can also be seen with an *m/z* of 1829.893. The MIC of compound **2.9** was found to be 1.25 μg/mL. This study revealed two very important things. One is that the ketone group in the 4'-methyl-4-benzoylbenzaldehyde substrate was not affected during the reductive amination reaction. The second is that the presence of the methyl group at the 4-position in the benzophenone unit of **2.9** did not appear to affect activity.

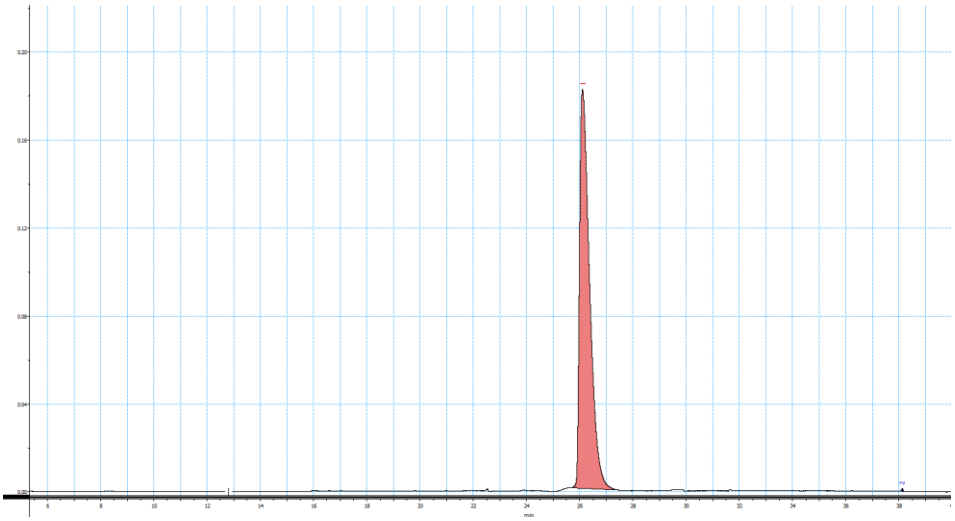

Figure 2.12. Analytical HPLC trace to confirm the purity of the Dap derivative **2.9**

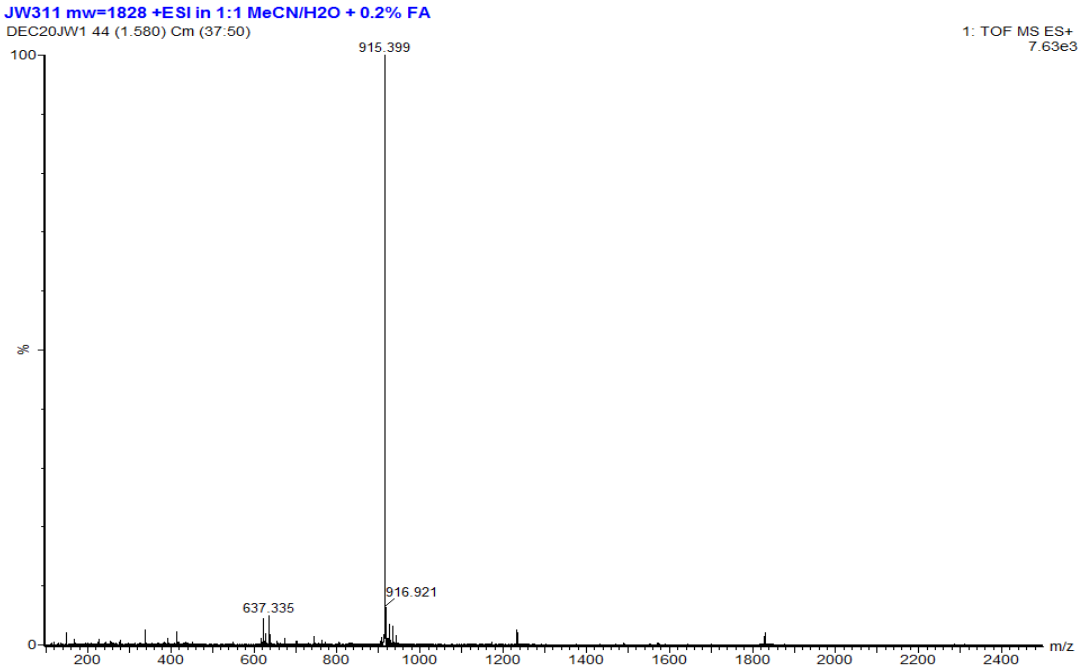

Figure 2.13. ESI^+ mass spectra of compounds **2.9**

2.3.3 Effect of the Alkyne Tail on Dap Activity

The last study we performed before attempting the synthesis of the Dap-PAL was to determine if the alkyne tail would affect Dap activity. The Dap derivative that we designed in order

to test this is compound **2.11** (figure. 2.14). How we arrived at **2.11** is described as follows. In order to find out how the alkyne would affect activity, we would first need to design a way to attach it to the free amino group of ornithine. The best way to do this is through, as we had found through the above investigations, was a reductive amination, meaning that our non-peptide substrate would have to contain an aldehyde. We would want the alkyne to be roughly equally as far from Dap as is in our proposed label **2.1** however we could not use a benzophenone spacer, as we are only interested in knowing how the alkyne affects activity alone. Knowing from literature review that attaching a biphenyl group to the ornithine residue through reductive amination has a very small effect on activity, we decided to use that as a linker to the alkyne group, as it would roughly result in the same amount of space between Dap and the alkyne as in compound **2.1**. We also anticipated that the non-peptide substrate required to obtain **2.12** would be straightforward to prepare.

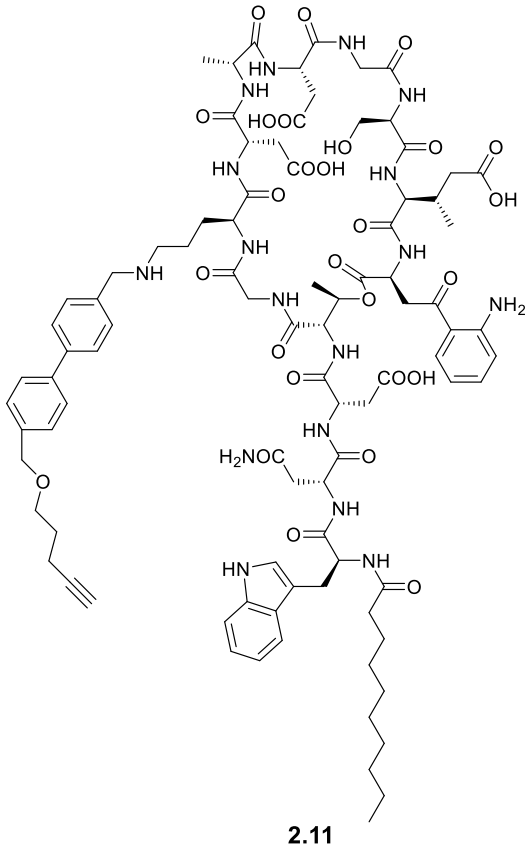

2.11

Figure 2.14. Structure of Dap analog **2.11**.

The synthesis of compound **2.12**, which is the non-peptide substrate required to prepare **2.11**, is outlined in Scheme 2.7. The synthesis began with a Suzuki coupling between 4-bromobenzaldehyde and TBDMS-protected 4-hydroxyphenylboronic acid in the presence of a catalytic amount of tetrakis(triphenylphosphine)palladium in ethylene glycol dimethyl ether and four equivalents sodium carbonate.[111] This gave compound **2.13** in a yield of 84%. Alongside this reaction, 4-pentyn-1-ol was reacted with methanesulfonyl chloride in the presence of triethylamine which gave compound **2.14** in a 70% yield.[112] Reaction of **2.14** with **2.13** in dry DMF in the presence of potassium carbonate gave **2.11** in a 95% yield.[113] Compound **2.12** was attached to the Orn residue of Dap using our usual reductive amination procedure.[108] After purification by semi-preparative RP-HPLC compound **2.11** was obtained in a 40% yield. An

analytical HPLC chromatogram of **2.11** after preparative HPLC (figure 2.15) showed one peak confirming its purity. In the ESI+ mass spectrum of **2.11** the doubly positive charged ion was dominant (*m/z* peak at 935.406, figure 2.16). The singly charged species can also be seen with an *m/z* of 1869.85. The MIC of compound **2.11** was found to be 2.0 μg/mL which indicates that the alkyne tail does not significantly alter Dap activity.

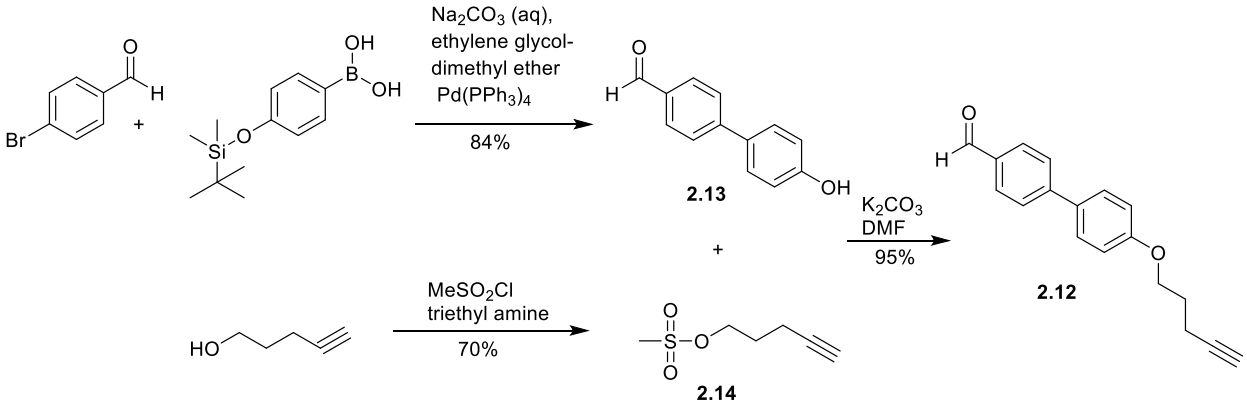

Scheme 2.7. Synthesis of compound **2.12**.[111,112,113]

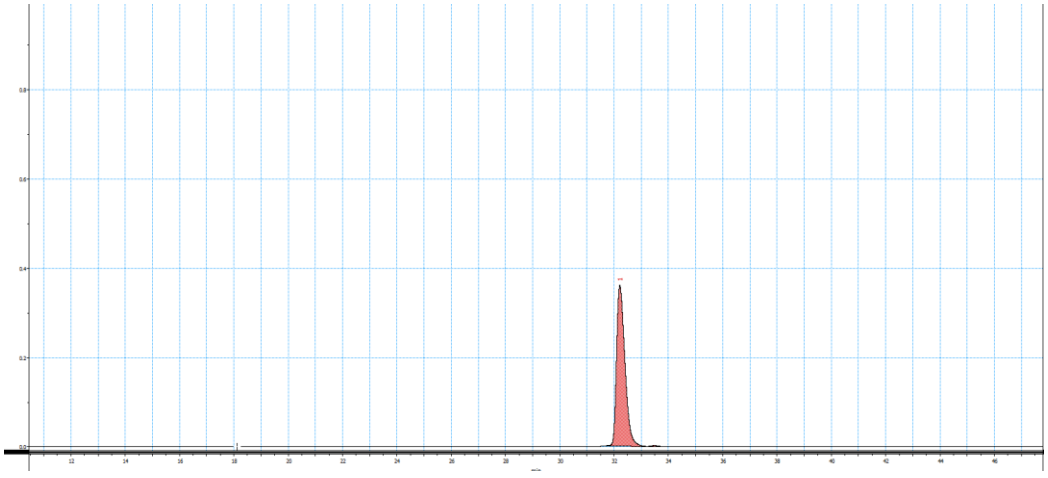

Figure 2.15. HPLC analytical trace to check purity of compound **2.11.**

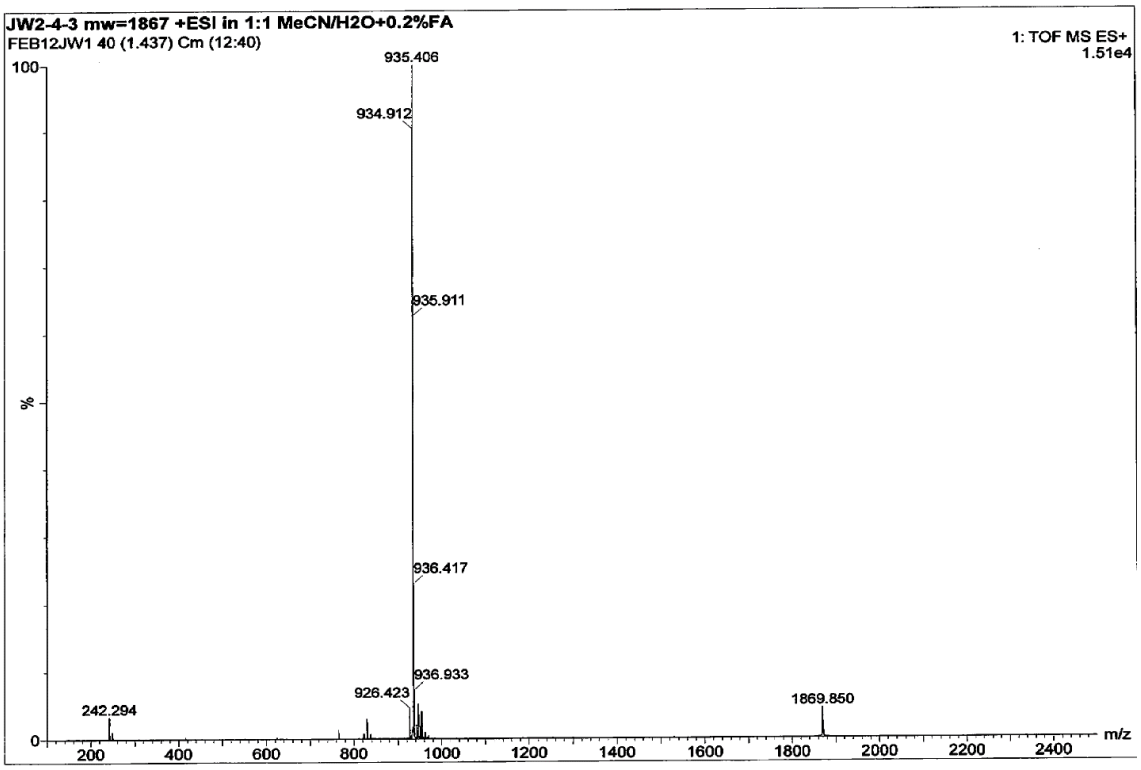

Figure 2.16. ESI^+ mass spectra of compounds **2.11.**

2.3.4. Synthesis of a Dap-PAP

To summarize the findings of our previous studies, we now know that when attaching a compound to the ornithine residue of Dap, doing such through an amine linkage rather than an amide linkage results in better antibacterial activity of the compound. We also know that we can use a benzophenone based photoaffinity probe and still retain a large amount of antibacterial activity. What we also know that the point of substitution on the ring of the benzophenone is not an issue, as both the 3- and 4-substituted benzophenones resulted in roughly the same antibacterial activity with the 4-position being just slightly better than the 3-position. The last thing that we were able to deduce from the above studies was that including an alkyne tail on our benzophenone photoactive group should not significantly reduce activity. With the above information, we were

able to design the photoaffinity probe that would be used for our photoaffinity labeling study, compound **2.15** (figure 2.17).

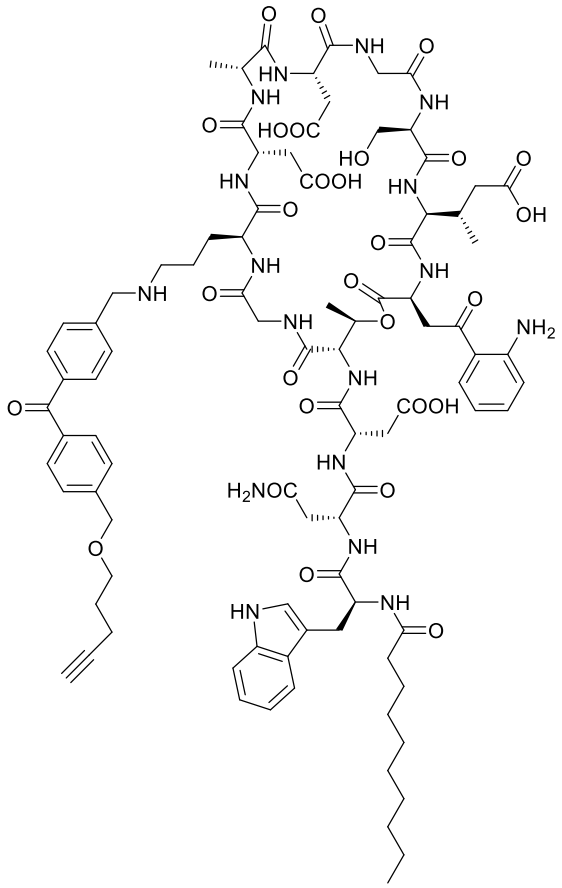

2.15

Figure 2.17. Structure of the proposed Dap photoaffinity probe.

The preparation of **2.15** required the synthesis of aldehyde **2.16** (figure 2.18). A retro synthesis of compound **2.16** is shown in scheme 2.8. The first bond to break was the ketone group in the benzophenone moiety. This bond could be made through a modified Suzuki

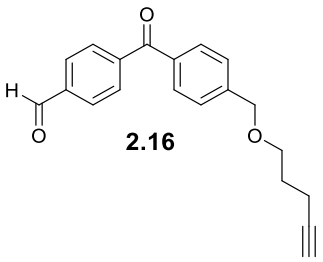

Figure 2.18. Structure of aldehyde **2.16**.

coupling by reacting compound **2.16** with 4-formylphenylboronic acid under the conditions as described by L.J. Gooben *et al*.[110] When looking at how to synthesize compound **2.17**, the best place to cleave would be the ether bond linkage. This bond could be synthesized by reacting *t*-butyl-protected 4-(bromomethyl)benzoic (**2.18**) acid with 4-pentyn-1-ol.

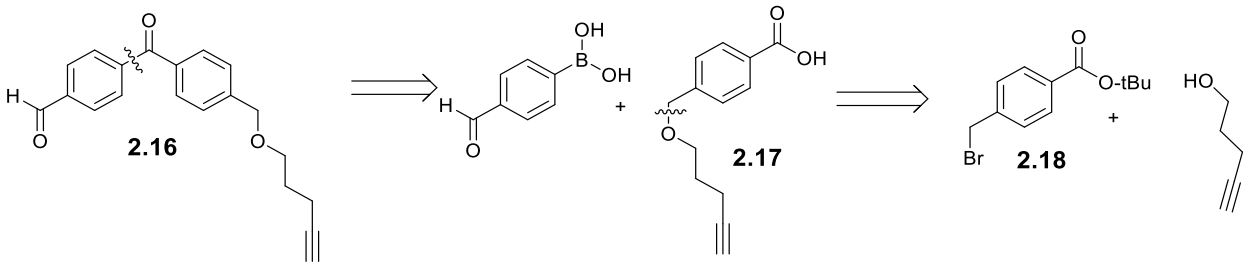

Scheme 2.8. Retrosynthetic analysis of compound **2.16**

The attempted synthesis of **2.16** via the route outlined in scheme 2.8 is outlined in scheme 2.9. The first compound to synthesize was compound **2.18**. *tert*-Butanol was reacted with p-toluoyl chloride in pyridine four days which gave compound **2.19** in a 55% yield.[114] Free radical bromination of **2.19** using azobisisobutyronitrile (AIBN), and N-bromosuccinimide (NBS) in refluxing benzene gave **2.18** in a 45% yield.[115] Appending 4-pentyn-1-ol to **2.18** turned out to be challenging. Numerous attempts to obtain **2.20** via reaction of the sodium alkoxide of 4-pentyn-1-

ol with **2.18** in dry THF did not result in the formation of any **2.20**.[116] Eventually we obtained **2.20** by adding NaH to neat 4-pentyn-1-ol (10 fold excess) and stirring the mixture for two hours. To this was added compound **2.18** and the mixture was stirred for 24 hours. This gave compound **2.20** in a 37% yield. The next step in the reaction process was to remove the *tert*-butyl protecting group in **2.20**. We first attempted this using 50% v/v trifluoroacetic acid (TFA) in methylene chloride and stirring for 24 hours.[117] Surprisingly, no reaction occurred. However, by using 4.0 M HCl in dioxane we were able to obtain compound **2.17** in excellent yield.[117] Now that we had compound **2.17**, we were able to attempt our modified Suzuki coupling. Compound **2.17**, $Pd(Ph_3)_4$, 4-formylphenylboronic acid, and dimethyl dicarbonate in dioxane were reacted in a Schlenk tube at 80˚C for 18 h.[110] However, no reaction took place. Therefore we decided to alter our synthetic strategy.

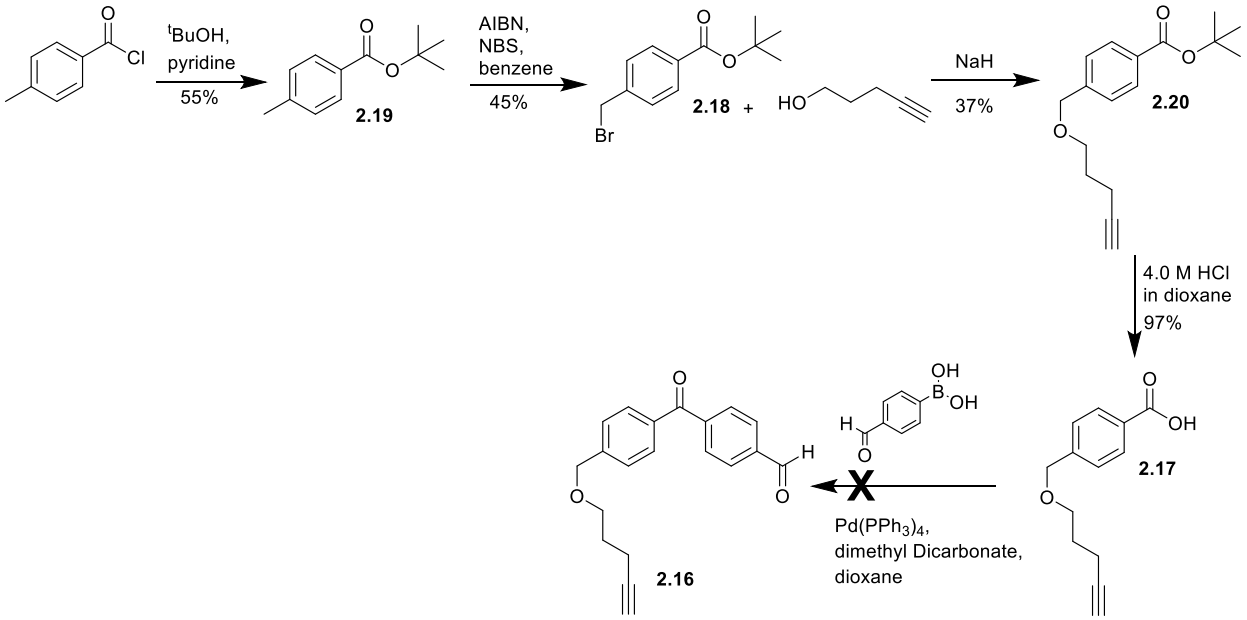

Scheme 2.9. First attempted synthesis of compound **2.16.**[110,114-117]

Another retrosynthesis of **2.16** is shown in scheme 2.10. Here the aldehyde is introduced at the end of the synthesis from compound **2.21**. Compound **2.21** is obtained for the reaction of 4,4'-(dibromomethyl)benzophenone (compound **2.22**), a literature compound, and 4-pentyn-1-ol.

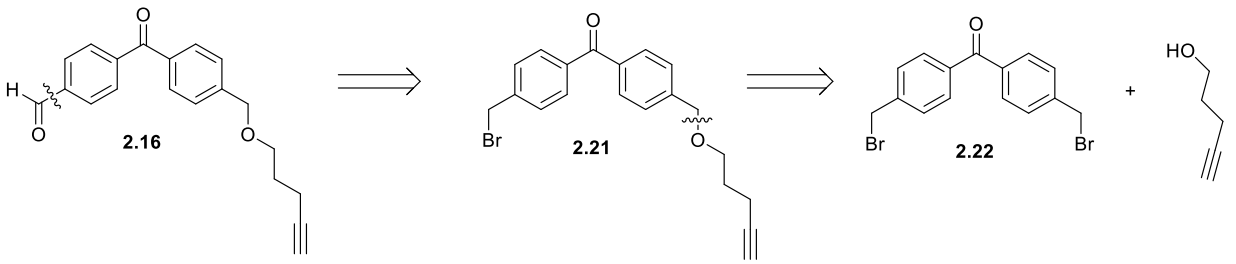

Scheme 2.10. Second retrosynthetic analysis of compound **2.16.**

The second attempted synthesis of compound **2.16** is outlined in scheme 2.11. 4,4'-(dibromomethyl)benzophenone (compound **2.22**) was prepared in a 37 % yield via free radical bromination of 4,4'-dimethylbenzophenone using cat. benzoyl peroxide and *N*-bromosuccinimide (NBS) as described by Wang et al.[118] To couple the alcohol to **2.22** we performed the reaction neat by adding 1 equiv (to compound **2.22**) of sodium hydride to an excess of 4-pentyn-1-ol. After stirring for one hour compound **2.22** was added and the resulting mixture was stirred 18h. Upon workup and purification via column chromatography compound **2.21** was obtained in a 21% yield.[116] Compound **2.21** was then dissolved in dioxane, and to this solution was added a 0.7 M solution of calcium carbonate in water. The resulting mixture was refluxed overnight, and upon workup and purification via column chromatography compound **2.23** was produced in a 45% yield.[119] Compound **2.23** was then dissolved in methylene chloride, and pyridinium chlorochromate (PCC) was added to the solution. The solution was then stirred at -20˚C overnight. Upon workup, and purification via column chromatography compound **2.16** was obtained in a 76% yield.[120]

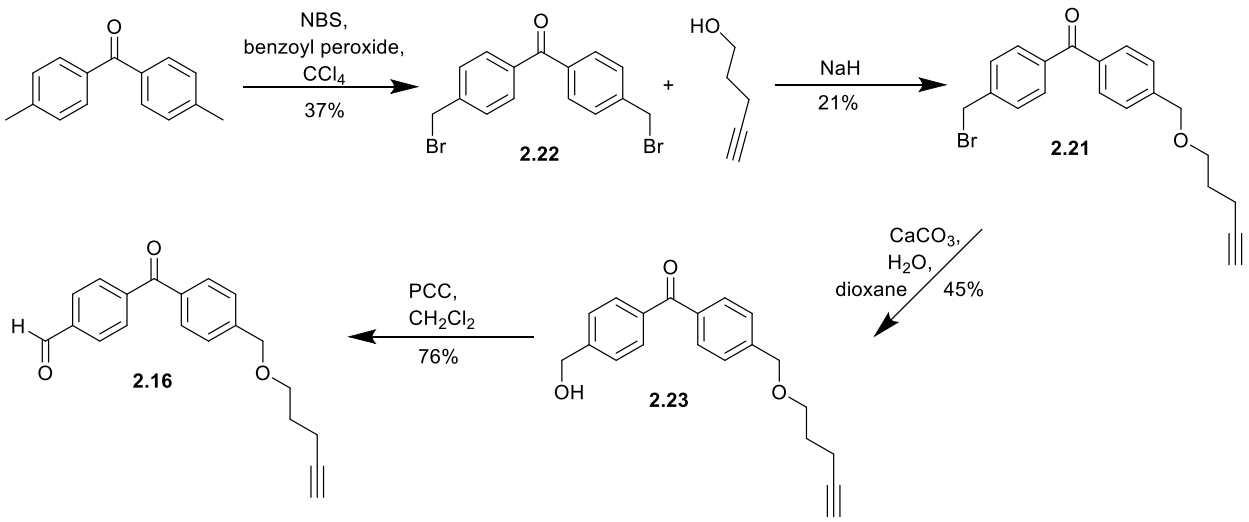

Scheme 2.11. Synthesis of our target compound **2.16**[116-120]

Compound **2.16** was attached to the Orn residue of Dap using our usual reductive amination procedure. After purification by semi-preparative RP-HPLC compound **2.15** was obtained in a 22% yield.[108] An analytical HPLC chromatogram of **2.15** after preparative HPLC (figure 2.19) showed one peak confirming its purity. In the ESI+ mass spectrum of **2.15** the doubly positive charged ion was dominant (*m/z* peak at 955.841, figure 2.20). The singly charged species can also be seen with an *m/z* of 1911.745. The MIC of compound **2.15** was found to be 1.5 μg/mL which is only two times greater than the MIC of Dap.

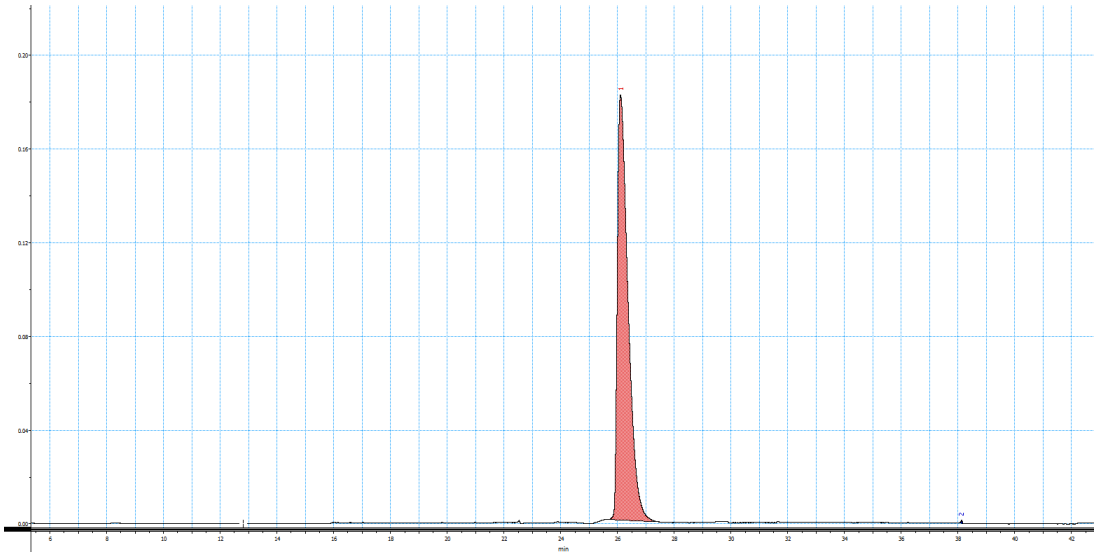

Figure 2.19. HPLC analytical trace to confirm purity of Dap derivative **2.15**

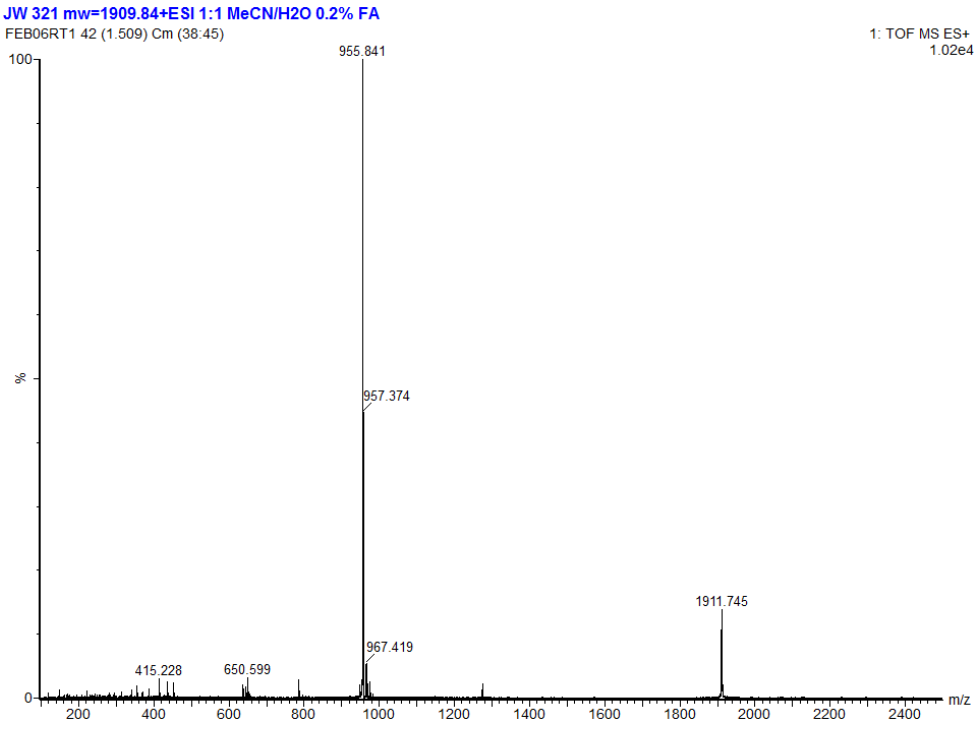

Figure 2.20. ESI^+ mass spectra of compounds **2.15**

2.4 Conclusions and Future Work

A series of Dap derivatives modified at the free amino group of the ornithine residue were synthesized and examined for antibacterial activity in order to design the best possible Dap-PAP. During these studies, it was found that attaching compounds via an amine linkage was more efficient at retaining antibacterial activity than via an amide linkage. This was shown when comparing compounds **2.2** and **2.3** with each other. We found that a benzophenone group as a photoactive group was suitable for our design, as a good amount of activity was retained, and that attaching the benzophenone via the para position yielded slightly better activity compared to a meta linkage. This was found through comparing compounds **2.5** and **2.6**. We also found out that when attaching the benzophenone group via reductive amination, there was no unwanted reduction of the ketone group, as was shown in the investigation of compound **2.9**. We had also found that adding an alkyne based tail did not adversely affect the antibacterial activity of our photolabel, as was shown in the investigation of compound **2.11**. Armed with this knowledge, we were able to synthesize our proposed photoactive group, compound **2.16**, and subsequently attach it to Dap via reductive amination to give compound **2.15**. This photoprobe derivative of Dap retained much of Dap's antibacterial activity in the presence of *B. subtilis* having an MIC of 1.5μg/mL.

Having synthesized this compound, there is still much future work to be done with this compound. The next step is to perform the photoaffinity labelling studies using the method as set forth by Eirich *et al*. in their very similar study performed on vancomycin. With this, it is hoped that the protein or lipid with which Dap interacts with in the membrane can be identified through MS studies.

2.5 Experimental

2.5.1 General

DMF was distilled under reduced pressure from CaH. 1,4-dioxane was distilled from $CaCl_2$. Pyridine was distilled from KOH. Benzene was distilled from $CaCl_2$. Methylene chloride and THF were attained from a PurSolv dry solvent purification system. All reagents used in syntheses were purchased from Sigma Aldrich Chemical Co (Milwaukee, Wisc., USA). Daptomycin was a gift from Cubist Inc. (Boston, Mass., USA). Flash chromatorgraphy was performed using 60 Å (324-400 mesh) silica gel purchased from Silicycle (Laval, Quebec, Canada). ^{1}H-NMR and ^{13}C-NMR were performed on a Bruker Advance 300, and chemical shifts are reported relative to the internal standard tetramethylsilane (TMS) in ppm. Positive ion electrospray mass spectrometry (+ESI) was performed on a Waters/Micromass QTOF Ultima Global mass spectrometer using 1:1 MeOH/H_2O (0.1% FA) as solvent. Analytical and semi-preparative HPLC was performed on a Waters 600E system equipped with a Waters 474 scanning fluorescence detector ($\lambda_{excitation}$ = 356 nm, $\lambda_{emission}$ = 460 nm). Semi-preparative HPLC was performed using a Higgins (Higgins Analytical Inc., Mountainview, CA., USA) Proto-200 C-18 semi-preparative (20 mm x 250 mm) column with a flow rate of 6 mL/min. Analytical HPLC was performed using a Phenomenex (Torrance, CA., USA) Jupiter Proteo C-18 analytical (4.6 mm x 250 mm) column with a flow rate of 1 mL/min.

2.5.2. Syntheses

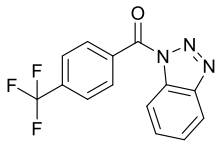

Compound 2.4.[106] To a solution of benzotriazole (3.81 g, 32.0 mmol) in dry CH_2Cl_2 (40 mL) under nitrogen was added a solution of thionyl chloride (0.96 g, 8.0 mmol) in dry CH_2Cl_2 (10 mL) over 3 minutes. After stirring for 30 minutes 4-trifluoromethyl benzoic acid (1.52 g, 8.00 mmol) was added. The mixture was stirred for 4 hours at room temperature, and the resulting precipitate was removed by filtration. The filter cake was washed with CH_2Cl_2 (50 mL). The combined organic layers were washed with aq. NaOH (0.4 M, 2 x 50 mL) and water (2 x 50 mL). The organic layer was then dried (Na_2SO_4), concentrated and purified via silica gel flash chromatography (95:5 Hex:EtOAc) to yield 1.475g (65%) of compound **2.4**. ^{1}H-NMR ($CDCl_3$): δ7.65 (t, J = 7.9 Hz, 1H), 7.77 (t, J = 7.9 Hz, 1H), 7.86 (d, J = 8.0 Hz, 2H), 8.22 (d, J = 8.0 Hz, 1H), 8.39 (d, J = 7.8 Hz, 2H), 8.45 (d, J = 7.9 Hz, 1H)

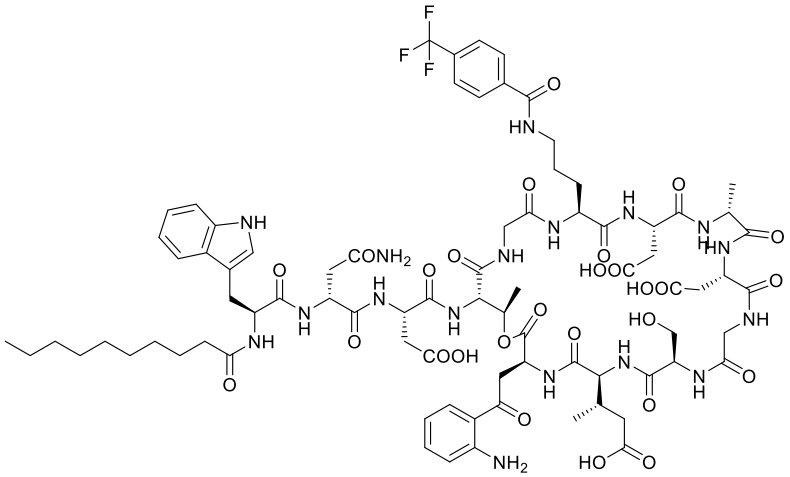

Compound 2.2. To a solution of Dap (200 mg, 0.124 mmol) dissolved in dry DMF (5mL) was added of compound 2.4 (43 mg, 0.147 mmol), and the resulting mixture was stirred at room

temperature for 24 hours in a dry sintered glass vial, under nitrogen. The mixture was then diluted with 0.1% TFA solution in water (5 mL), and purified via HPLC to yield 100mg (45%) of compound **2.2**. Compound **2.2** yielded a minimum inhibitory concentration (MIC) of 3μg/mL using the procedure described in section 2.5.3. MS (+ESI): m/z = 896.871. HRMS (+ESI): $C_{80}H_{105}N_{17}O_{27}F_3$.

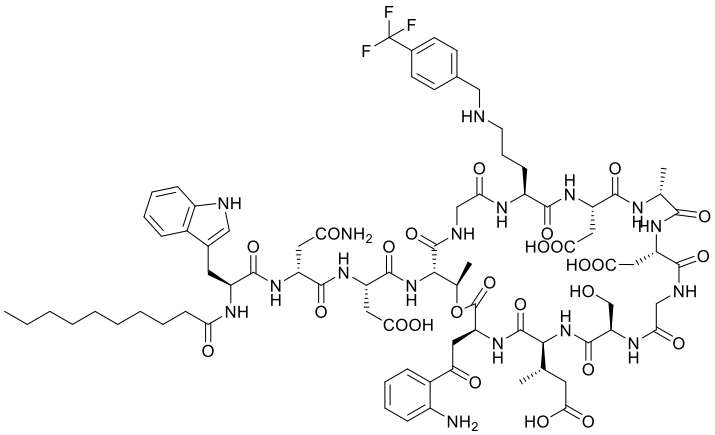

Compound 2.3. To a solution of Daptomycin (200 mg, 0.124 mmol) in dry DMF (5 mL) was added 4-(trifluoromethyl)benzaldehyde (44 mg, 0.248mmol), sodium triacetoxyborohydride (52 mg, 0.248 mmol), and glacial acetic acid (300 μL). This mixture was stirred at room temperature for 24 hours in a dry sintered glass vial, under argon. The mixture was then diluted with 0.1% TFA solution in water (5 mL), and purified via HPLC to yield 34.1mg (16%) of compound **2.3**. Compound **2.3** yielded a minimum inhibitory concentration (MIC) of 2 μg/mL using the procedure described in section 2.5.3. MS (+ESI): m/z = 890.351. HRMS (+ESI): $C_{80}H_{107}N_{17}O_{26}F_3$.

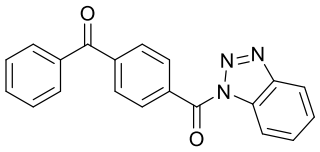

Compound 2.7. To a solution of benzotriazole (1.06 g, 8.84 mmol) dissolved in dry CH_2Cl_2 (10 mL), under nitrogen, was added thionyl chloride (0.263 g, 2.21 mmol), dissolved in dry CH_2Cl_2 (5 mL), over 3 minutes. After stirring for 30 minutes, 4-benzoylbenzoic acid (0.500 g, 2.21 mmol) was added. The mixture was stirred for 4 hours at room temperature, and the resulting precipitate was removed by filtration. The filter cake was washed with CH_2Cl_2 (50 mL). The combined organic layers were washed with aq. NaOH (0.4 M, 2 x 50 mL) and water (2 x 50 mL). The organic layer was then dried (Na_2SO_4), concentrated and purified via silica gel flash chromatography (95:5 Hex:EtOAc) to yield 502mg (70%) of compound **2.7**. ^{1}H-NMR ($CDCl_3$): δ7.47 (m, 4H), 7.63 (ddd, J = 8.25 Hz, 7.17 Hz, 1.06 Hz, 1H), 7.75 (m, 2H), 7.85 (m, 2H), 8.08 (dt, J = 8.26 Hz, 0.90 Hz, 1H), 8.21 (m, 2H), 8.31 (m, 1H). ^{13}C-NMR ($CDCl_3$): δ115.04, 120.60, 126.90, 128.80, 129.88, 130.43, 130.96, 131.78, 132.41, 133.38, 134.73, 136.97, 141.95, 146.08, 166.33, 195.96. MS (+ESI): m/z = 328.10801. HRMS (+ESI): $C_{20}H_{14}O_2N_3$

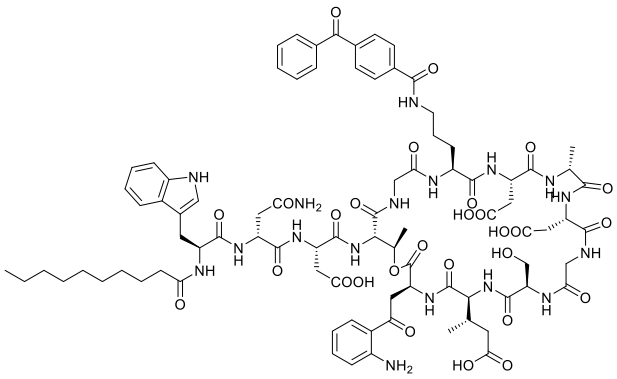

Compound 2.5. To a solution of Dap (50 mg, 0.031 mmol) dissolved in dry DMF (2 mL) was added compound **2.7** (12.2 mg, 0.0372 mmol), and the resulting mixture was stirred at room

temperature for 24 hours, under nitrogen. The mixture was then diluted with 0.1% TFA solution in water (2 mL), and purified via HPLC to yield 18.14mg (32%) of compound **2.5**. Compound **2.5** yielded a minimum inhibitory concentration (MIC) of 3μg/mL using the procedure described in section 2.5.3. MS (+ESI): m/z = 915.3898. HRMS (+ESI): $C_{86}H_{111}O_{28}N_{17}$.

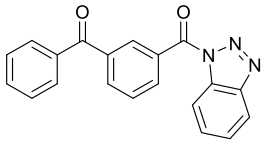

Compound 2.8. To a solution of benzotriazole (1.06 g, 8.84 mmol) dissolved in dry CH_2Cl_2 (10 mL), under nitrogen, was added thionyl chloride (0.263 g, 2.21 mmol), dissolved in dry CH_2Cl_2 (5 mL), over 3 minutes. After stirring for 30 minutes, 3-benzoylbenzoic acid (0.500 g, 2.21 mmol) was added. The mixture was stirred for 4 hours at room temperature, and the resulting precipitate was removed by filtration. The filter cake was washed with CH_2Cl_2 (50 mL). The combined organic layers were washed with aq. NaOH (0.4 M, 2 x 50 mL) and water (2 x 50 mL). The organic layer was then dried (Na_2SO_4), concentrated and purified via silica gel flash chromatography (95:5 Hex:EtOAc) to yield 464 mg (65%) of compound **2.8**. ^{1}H-NMR ($CDCl_3$): δ7.45 (m, 4H), 7.61 (m, 2H), 7.76 (m, 2H), 8.04 (m, 2H), 8.26 (dt, J = 8.28 Hz, 0.90 Hz), 8.31 (ddd, J = 7.83 Hz, 1.73 Hz, 1.27 Hz), 8.47 (m, 1H). ^{13}C-NMR ($CDCl_3$): δ114.98, 120.54, 126.83, 128.80, 129.00, 130.43, 130.90, 131.92, 132.38, 133.23, 133.47, 134.86, 135.30, 136.98, 138.02, 146.06, 166.23, 195.48. MS (+ESI): 328.10802. HRMS (+ESI): $C_{20}H_{14}O_2N_3$.

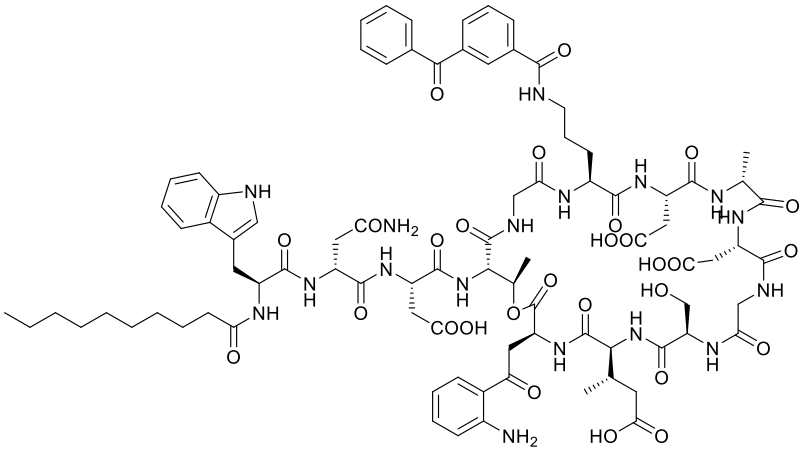

Compound 2.6. To a solution of Dap (50 mg, 0.031 mmol) dissolved in dry DMF (2 mL) was added compound **2.7** (12.2 mg, 0.0372 mmol), and the resulting mixture was stirred at room temperature for 24 hours, under nitrogen. The mixture was then diluted with 0.1% TFA in water (2 mL), and purified via HPLC to yield 19.8 mg (35%) of compound **2.6**. Compound **2.6** yielded a minimum inhibitory concentration (MIC) of 2.5 μg/mL using the procedure described in section 2.5.3. MS (+ESI): m/z = 915.38985. HRMS (+ESI): $C_{86}H_{111}O_{28}N_{17}$.

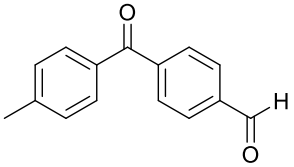

Compound 2.10.[110] Dry dioxane (50 mL) was degassed, in a dry Schlenk tube under argon, through a method of freezing in liquid nitrogen and subsequently evacuating the flask under vacuum, allowing it to melt, and refilling the Schlenk tube with argon. This was performed approximately 5 times, until bubbling upon melting had stopped. To the dioxane was added 4-formylbenzoic acid (1.92 g, 12.8 mmol), p-tolylboronic acid (2.09 g, 15.42 mmol), dimethyl dicarbonate (2.07 g, 15.4 mmol), and of tetrakis(triphenylphosphine)palladium (153 mg, 0.132 mmol), and the mixture was stirred at 80˚C for 6 hours. Upon completion, diethyl ether (100 mL),

and deionized water (100mL) was added. The layers were then separated, and the water layer was extracted with diethyl ether (2 x 100 mL). The organic layers were then combined, dried (Na_2SO_4), concentrated, and purified via silica gel flash chromatography was performed (95:5, Hex:EtOAc) to yield 1.07 g (40%) of compound **2.10**. ^{1}H-NMR ($CDCl_3$): δ2.34 (s, 3H), δ7.17 (d, J= 8.5 Hz, 2H, δ7.61 (d, J= 8.14 Hz, 2H), δ7.79 (d, J= 8.21 Hz, 2H). δ7.88 (d, J= 8.02 Hz, 2H), δ10.02 (s, 1H). MS (+ESI): m/z = 225.09101. HRMS (+ESI): $C_{15}H_{13}O_2$.

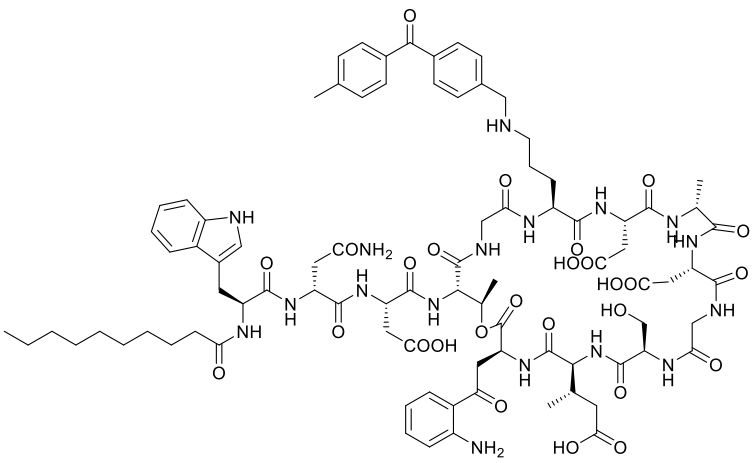

Compound 2.9. To a solution of Daptomycin (50 mg, 0.031 mmol) in dry DMF (2 mL) was added compound **2.10** (7.9 mg, 0.0372 mmol), sodium triacetoxyborohydride (13 mg, 0.062mmol), and glacial acetic acid (75 µL). This reaction mixture was stirred at room temperature for 24 hours in a dry sintered glass vial, under argon. The mixture was then diluted with 0.1% TFA solution in water (2 mL), and purified via HPLC to yield 13.1mg (22%) of compound **2.9**. Compound **2.9** yielded a minimum inhibitory concentration (MIC) of 1.3 µg/mL using the procedure described in section 2.5.3. MS (+ESI): m/z = 914.910. HRMS (+ESI): $C_{87}H_{114}O_{27}N_{17}$

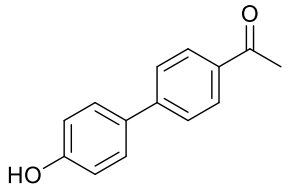

Compound 2.13.[111] To a solution of 4-bromobenzaldehyde (281 mg, 1.53mmol) in aq. Na_2CO_3 (2.0 M, 2.3 mL, 4.58 mmol) and ethylene glycol (2.5mL) was added 4-tertbutyldimethylsilyl-phenylboronic acid (500 mg, 1.98 mmol), and of tetrakis(triphenylphosphine)palladium (88 mg, 0.077 mmol), under nitrogen. The mixture was refluxed for 4 hours, and subsequently cooled to room temperature, diluted with water (10 mL), and extracted with ethyl acetate (3 x 10mL). The combined organic layers were dried (Na_2SO_4) and concentrated. The resulting residue was purified with silica gel flash chromatography (70:30 hex:EtOAc) to yield 254 mg (84%) of compound **2.13**. ^{1}H-NMR (DMSO-d_6): δ 6.74 (2H, d, J=8.61Hz), 7.49 (2H, d, J=8.63Hz), 7.69 (2H, d, J=8.32Hz), 7.80 (2H, d, J=8.28Hz), 9.65 (1H, s), 9.87 (1H, s).

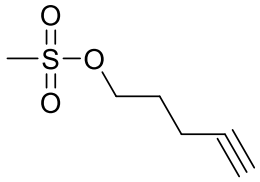

Compound 2.14.[112] To a solution of 4-pentyn-1-ol (910 mg, 10.8 mmol) in methylene chloride (15 mL) under nitrogen at 0˚C was added triethylamine (2.18 g, 21.5 mmol) and methanesulfonyl chloride (1.85 g, 16.1 mmol). The mixture was stirred at room temperature for 4h, and aq. ammonium chloride (sat., 10 mL) was added to quench the reaction. The aq. layer was extracted with methylene chloride (3 x 15 mL). The combined organic layers were washed with water (3 x 15 mL) dried (Na_2SO_4) and concentrated. Acetone was added to the resulting residue (3 x 20 mL) and concentrated remove trace triethylamine, to yield 1.23 g (70%) of compound **2.14**. ^{1}H-NMR

($CDCl_3$ – d_1): δ 1.82 (2H, m), 1.88 (1H, m), 2.23 (2H, dt, J=6.50, 2.2Hz), 2.90 (3H, s) 4.22 (2H, t, J=6.08Hz).

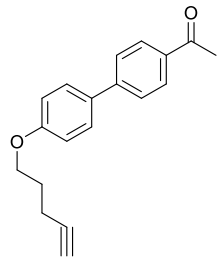

Compound 2.12. To a solution of potassium carbonate (238 mg, 1.72 mmol), and compound **2.14** (238 mg, 1.47 mmol) in DMF (5 mL) was added compound **2.13** (243 mg, 1.23 mmol), and stirred at 95˚C for 15 hours, with subsequent cooling to room temperature. Ethyl acetate (50 mL), and aq. sodium bicarbonate (sat., 50 mL) were then added. The aq. Layer was then extracted with ethyl acetate (3 x 50 mL), and the combined organic layers were washed with water (3 x 25 mL), dried (Na_2SO_4) and concentrated. The residue was then purified by silica gel flash chromatography (95:5 Hex:EtOAc) to yield 320 mg (96 %) of compound **2.12**. ^{1}H-NMR ($CDCl_3$): δ 1.87 (1H, t, J=2.63Hz), 1.93 (2H, m), 2.32 (2H, dt, J=6.95, 2.61Hz), 4.01 (2H, t, J=6.10Hz), 6.89 (2H, d, J=8.79Hz), 7.46 (2H, d, J=8.79Hz), 7.59 (2H, d, J=8.24Hz), 7.80 (2H, d, J=8.34Hz), 9.91 (1H, s). ^{13}C-NMR ($CDCl_3$): δ15.42, δ28.36, δ66.49, δ69.26, δ115.26, δ127.27, δ128.73, δ130.55, δ132.31, δ134.90, δ147.01, δ159.67, δ192.13. MS (+ESI): m/z = 265.1166. HRMS (+ESI): $C_{18}H_{16}O_2$.

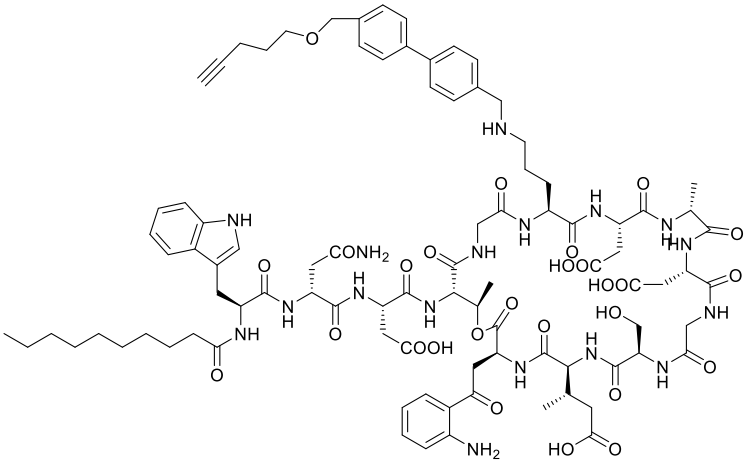

Compound 2.11. To a solution of Daptomycin (200 mg, 0.124 mmol) in dry DMF (5 mL) was added compound **2.12** (66 mg, 0.248 mmol), sodium triacetoxyborohydride (52 mg, 0.248 mmol), and glacial acetic acid (300μL). This reaction mixture was stirred at room temperature for 24 hours. This reaction mixture was stirred at room temperature for 24 hours in a dry sintered glass vial, under argon. The mixture was then diluted with 0.1% TFA solution in water (2 mL), and purified via HPLC to yield 92.5mg (40%) of compound **2.11**. Compound **2.11** yielded a minimum inhibitory concentration (MIC) of 2 μg/mL using the procedure described in section 2.5.3. MS (+ESI): m/z = 935.406. HRMS (+ESI): $C_{90}H_{118}N_{17}O_{27}$.

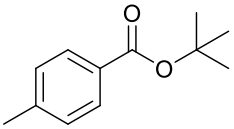

Compound 2.19.[114] To a solution of *tert*-butanol (970 mg, 13.1 mmol) in dry pyridine (2.0 mL) was added p-toluoyl chloride (2.00 g, 12.9 mmol), and the resulting mixture was stirred for 88 hours. The solution was diluted with water (4 mL) and ethyl acetate (4 mL). The organic layer was washed with aq. HCl (0.5 M, 3 x 2 mL), H_2O (3 x 2 mL), aq. sodium bicarbonate solution (sat., 3 x 2 mL), and aq. brine solution (sat., 3 x 2 mL). The organic layer was then collected, dried

(Na_2SO_4) and concentrated to yield 1.37 g (55%) of compound **2.19**. ^{1}H-NMR ($CDCl_3$): δ1.48 (s, 9H), δ2.28 (s, 3H), δ7.09 (d, J=7.90 Hz, 2H), δ7.77 (d, J=8.07Hz, 2H).

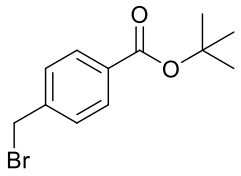

Compound 2.18.[115] To a solution of compound **2.19** (500 mg, 2.60 mmol) in dry benzene (20 mL) was added azobisisobutyronitrile (AIBN) (21 mg, 0.13 mmol) and N-bromosuccinimide (NBS) (509 mg, 2.86 mmol) under nitrogen. The mixture was stirred at reflux for 5 hours, cooled to R.T. and the resulting precipitate was removed by filtration. The filter cake was washed with benzene (20 mL). The filtrate was concentrated and purified via silica gel flash chromatography (95:5, hex:EtOAc) to yield 317 mg (45%) of compound **2.18**. ^{1}H-NMR ($CDCl_3$): δ1.61 (s, 9H), δ4.50 (s, 2H), δ7.44 (d, J=8.30 Hz, 2H), δ7.97 (d, J=8.32 Hz, 2H)

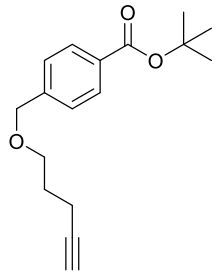

Compound 2.20. This procedure was modified from that which had previously been done by Sharma *et al.* A solution of NaH in mineral oil (60% by mass, 183 mg, 4.50 mmol) in neat 4-pentyn-1-ol (3.00 mL, 2.71 g, 32.2 mmol) was stirred for 2 hours. To the mixture was added of compound **2.18** (770 mg, 2.84 mmol), and the mixture was stirred for 14h. The mixture was diluted with diethyl ether (40 mL), and the organic layer was washed with H_2O (3 x 20 mL), and aq. brine (sat., 3 x 20 mL). The organic layer was then collected, dried (Na_2SO_4) and concentrated. The

resulting residue was purified via silica gel flash chromatography (98:2, Hex:EtOAc) to give 365 mg (46% yield) of compound **2.20**. ^{1}H NMR ($CDCl_3$): δ1.47 (s, 9H), δ1.72 (q, J=6.59 Hz, 2H), δ1.83 (t, J=2.66 Hz, 1H), δ2.21 (td, J=7.07 Hz, 2.65 Hz, 2H), δ3.46 (t, J=6.14 Hz, 2H), δ4.44 (s, 2H), δ7.25 (d, J=8.53 Hz, 2H), δ7.84 (d, J=8.39 Hz, 2H). ^{13}C NMR ($CDCl_3$): δ15.52, δ28.42, δ28.84, δ68.82, δ69.06, δ72.61, δ81.15, δ84.05, δ127.20, δ129.75, δ131.41, δ143.44, δ165.82. MS (+ESI): m/z = 275.1938. HRMS (+ESI): $C_{17}H_{23}O_3$.

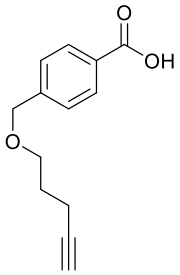

Compound 2.17. A solution of compound **2.20** (365 mg, 1.321 mmol) was stirred in a mixture of HCl in dioxane (4.0 M, 8.0 mL) overnight, and monitored by TLC. The solvent was removed under vacuum, and the residue was subsequently co-evaporated with toluene (4 x 10 mL) to yield 283mg (97 % yield) of compound **2.17**. ^{1}H-NMR ($CDCl_3$): δ1.74 (q, J=6.56 Hz, 2H), δ1.84 (t, J=2.66 Hz, 1H), δ2.23 (td, J= 7.09 Hz, 2.65 Hz, 2H), δ3.50 (t, J=6.13 Hz, 2H), δ4.48 (s, 2H), δ7.33 (d, J=8.47 Hz, 2H), δ7.97 (d, J=8.36 Hz, 2H). ^{13}C-NMR ($CDCl_3$): δ15.51, δ28.80, δ68.92, δ69.26, δ72.54, δ84.01, δ127.34, δ128.71, δ130.47, δ145.05, δ172.43. MS (+ESI): (m/z) = 219.10157. HRMS (+ESI): Composition = $C_{13}H_{15}O_3$

\

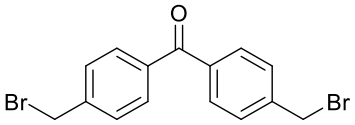

Compound 2.22.[118] To a solution of 4,4'-dimethylbenzophenone (1.60 g, 7.662 mmol) in CCl_4 (85 mL), in a dry 2-necked RBF under nitrogen, was added benzoyl peroxide (1.2 mg, 0.00075 mmol), and the mixture was heated to reflux. *N*-bromosuccinimide (3 x 1.0 g, 5.618 mmol) was then added to the solution with 15 minutes between each addition. Benzoyl peroxide (1.2 mg, 0.00075 mmol) was then added to the solution and refluxing continued for a further 14 h. The solution was allowed to cool to room temperature, and resulting precipitate filtered. The filter cake was then washed with CCl_4 (40 mL). The organic layer was washed with water (3 x 50 mL), dried (Na_2SO_4) and concentrated. A silica gel flash column (9:1 Hex:EtOAc) was used to purify the residue, yielding 2.08 g (74%) of compound **2.22**. ^{1}H-NMR ($CDCl_3$): δ 4.53 (s, 4H), 7.50 (d, 8.2 Hz, 4H), 7.77 (d, 8.1 Hz, 4H).

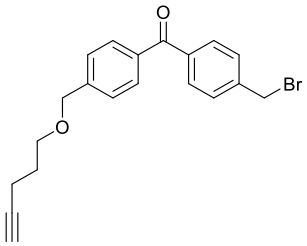

Compound 2.21. A solution of NaH in mineral oil (60% by mass, 135 mg, 3.38 mmol) in neat 4-pentyn-1-ol (7.0 mL, 6.32 g, 75.23 mmol) was stirred for 2 hours. To the mixture was added compound **2.22** (1.13 g, 3.07 mmol), and the mixture was stirred for 14 h. The mixture was diluted with diethyl ether (50 mL), and the organic layer was washed with H_2O (3 x 30 mL), and aq. brine (sat., 3 x 30 mL). The organic layer was then collected, dried (Na_2SO_4) and concentrated. The

resulting residue was purified via silica gel flash chromatography (95:5, Hex:EtOAc) to yield 0.319 g (28%) of compound **2.21**. ^{1}H-NMR: δ1.88 (q, J= 6.58 Hz, 2H), δ1.97 (t, J= 2.61 Hz, 1H), δ2.37 (td, J= 7.03 Hz, 2.61 Hz, 2H), δ3.65 (t, J= 6.14 Hz, 2H), δ4.56 (s, 2H), δ4.62 (s, 2H), δ7.50 (m, 4H), δ7.80 (m, 4H). ^{13}C-NMR ($CDCl_3$): δ15.52, δ28.87, δ33.64, δ68.77, δ69.22, δ72.60, δ126.21, δ127.34, δ130.46, δ130.60, δ137.04, δ142.16, δ143.55, δ169.26. MS (+ESI): m/z = 371.06471. HRMS (+ESI): $C_{20}H_{20}O_2Br$.

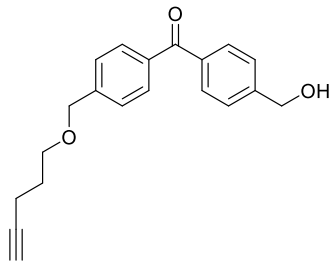

Compound 2.23. To a solution of calcium carbonate (585 mg, 5.84 mmol) in water (5 mL) was added a solution of compound **2.21** (425 mg, 1.15 mmol) in dioxane (5 mL), and the mixture was refluxed for 14 h. Upon cooling, dichloromethane (20 mL) and water (20 mL) were then added. The aq. layer was acidified with HCl at 0˚C to pH 5 and extracted with dichloromethane (3 x 10 mL). The organic layers were combined, dried (Na_2SO_4) and concentrated. Purification of the residue was performed via silica gel flash chromatography (50:50 Hex:EtOAc) to yield 158 mg (45%) of compound **2.23**. ^{1}H NMR ($CDCl_3$): δ1.74 (q, J=6.54 Hz, 2H), δ1.84 (s, 1H), δ1.96 (broad s, 1H), δ2.23 (td, J= 6.96 Hz, 2.03 Hz, 2H), δ3.51 (t, J=6.05 Hz, 2H), δ4.48 (s, 2H), δ4.68 (s, 2H), δ7.34 (m, 4H), δ7.66 (m, 4H). ^{13}C NMR ($CDCl_3$): δ15.52, δ28.82, δ64.92, δ68.87, δ69.27, δ72.62, δ126.64, δ127.33, δ130.46, δ130.60, δ137.04, δ143.56, δ145.76, δ169.42. MS (+ESI): m/z = 309.14844. HRMS (+ESI): $C_{20}H_{21}O_3$

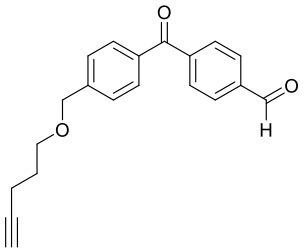

Compound 2.16. To a solution of compound **2.23** (100 mg, 0.3243 mmol) in dichloromethane (5 mL), cooled to -20˚C, was added pyridinium chlorochromate (PCC) (77 mg, 0.3567 mmol) and the solution was stirred at -20˚C for 1 hour. The solution was then concentrated, and purified via silica gel flash chromatography (80:20 Hex:EtOAc) to yield 75.5 mg (76%) of compound **2.16**. ^{1}H-NMR ($CDCl_3$): δ1.75 (q, J=6.58 Hz, 2H), δ1.84 (t, J=2.58 Hz, 1H), δ2.23 (td, J= 7.02 Hz, 2.62 Hz, 2H), δ3.52 (t, J= 6.12 Hz, 2H), δ4.50 (s, 2H), δ7.36 (d, J= 8.09 Hz, 2H), δ7.68 (d, J= 8.12 Hz, 2H), δ7.80 (d, J= 8.20 Hz, 2H), 7.88 (d, J= 8.16 Hz, 2H). ^{13}C-NMR ($CDCl_3$): δ15.51, δ28.80, δ68.89, δ69.35, δ72.52, δ127.47, δ129.75, δ130.53, δ130.57, δ136.11, δ138.67, δ142.89, δ144.44, δ191.92, δ195.76. MS (+ESI): m/z = 307.1416. HRMS (+ESI): $C_{20}H_{19}O_3$.

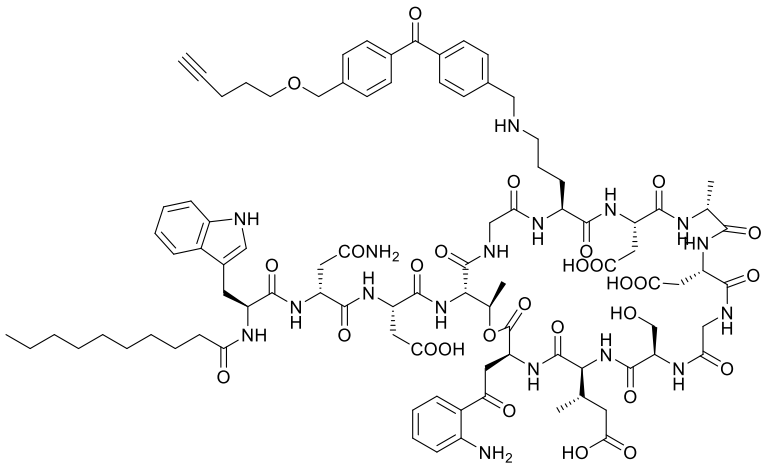

Compound 2.15. To a solution of Daptomycin (50 mg, 0.031 mmol) in dry DMF (2 mL) was added compound **2.16** (12 mg, 0.0372 mmol), sodium triacetoxyborohydride (13 mg, 0.062 mmol), and glacial acetic acid (75 μL). This reaction mixture was stirred at room temperature for 24 hours in a dry sintered glass vial, under argon. The mixture was then diluted with 0.1% TFA solution in water (2 mL), and purified via HPLC to yield 13.1mg (22%) of compound **2.15**. Compound **2.15** yielded a minimum inhibitory concentration (MIC) of 1.5 μg/mL using the procedure described in section 2.5.3. MS (+ESI): m/z = 955.8410. HRMS (+ESI): $C_{90}H_{119}O_{27}N_{20}$

2.5.3 Determination of MICs

The following protocol for activity testing using *B. subtilis* has been adapted from the procedure perfomed by *Muriah et al.*[109] All of the following was done using aseptic techniques (flaming all test tubes/utensils before and after addition, autoclaving/drying all tubes/media before use and using new pipette tips for each addition to all solutions).

A test tube containing 2 mL of a 20 g/L LB solution without calcium is inoculated with a glycerol stock solution of *B. subtilis* cells. The tube is placed in a shaker and shaken for 18 h (33-

37 ˚C at 150 rpm). The test tubes are removed from the shaker. Bacterial growth is evident by the cloudiness of the solution.

Approximately 0.40 mg of Dap or Dap derivative was dissolved in 10 μL of DMF and subsequently diluted with H_2O in order to make a 1 mg/mL solution. This solution is diluted with water to give a 50 μg/mL stock solution of Dap or Dap derivative. 5-100 μL of the stock solution of Dap or Dap analogue was added to a test tube containing 20 g/L LB media containing 5 mM Ca^{2+} such that the total volume is 995 μL. To this was added 5μL of the *B. subtilis* cell solution and then shaken for 18 h. The tubes are then inspected visually for cell growth. A clear solution indicated no cell growth. The MIC was the concentration of antibiotic that prevented cell growth as determined by the clear solution. All determinations were performed in triplicate.

References

1. Jovetic, S.; Zhu, Y.; Marcone, G. L.; Tramper, J. *Trends Biotech.* **2010,** *28,* 596-604.

2. Hiramatsu, K.; Hanaki, H.; Ino, T.; Yabuta, K.; Oguri, T.; Tenover, F. C. *J. Antimicrob. Chemother.* **1997,** *40,* 135-136.

3. Baltz, R. H.; Maio, V.; Wrigley, S. K. *Nat. Prod. Rep.* **2005,** *22,* 717-741.

4. Baltz, R. H. *Microbe* **2007,** *2,* 125-131.

5. Boeck, L. D.; Fukuda, D. S.; Abbott, B. J.; Debono, M. J. *J. Antibiot.* **1988,** *41,* 1085-1092.

6. Kreuzman, A. J.; Hodges, R. L.; Swartling, J. R.; Pohl, T. E.; Gahg, S. K.; Baker, P. J.; McGilvray, D.; Yeh, W. K. *Ind. Microbiol. Biotechnol.* **2000,** *24,* 173-180.

7. Woodworth, J. R.; Nyhart Jr, E. H.; Brier, G. L.; Wolny, J. D.; Black, H. R. *Antimicrob. Agents Chemother.* **1992,** *36,* 318-325.

8. Tally, F. P.; Zeckel, M.; Wasilewski, M. M.; Carini, C.; Berman, C. L.; Drusano, G. L.; Oleson Jr, F. B. *Expert Opin. Invest. Drugs* **1999,** *8,* 1223-1238.

9. Einstein, B. I.; Oleson Jr, F. B.; Baltz, R. H. *Clin. Infect. Dis.* **2010,** *50 (Supplement 1),* S10-S15.

10. Oleson Jr, F. B.; Berman, C. L.; Kirkpatrick, J. B.; Regan, K. S.; Lai, J. J.; Tally, F. P. *Antimicrob. Agents Chemother.* **2000,** *44,* 2948-2953.

11. Maio, V.; Coeffet-Legal, M. F.; Brian, P.; Brost, R.; penn, J.; Whiting, A.; Martin, S.; Ford, R.; Parr, I.; Bouchard, M.; Silva, C. J.; Wrigley, S. K.; Baltz, R. H. *Microbiology* **2005,** *151,* 1507-1527.

12. Malhert, C.; Kopp, F.; Thirlway, J.; Micklefield, J.; Marahiel, M. A. *J. Am. Chem. Soc.* **2007,** *129,* 12011-12018.

13. Whitman, M.; Linne, U.; Pohlmann, V.; Marahiel, M. A. *FEBSJ* **2008,** *285,* 5343-5354.

14. Robbel, L.; Marahiel, M. A. *J. Biol. Chem.* **2010,** *285,* 27501-27508.

15. Marahiel, M. A.; Essen, L. O. *Methods Enzymol.* **2009,** *458,* 337-351.

16. Marahiel, M. A. *J. Pept. Sci.* **2009,** *2009,* 799-807.

17. Fischbach, M. A.; Walsh, C. T. *Chem. Rev.* **2006,** *106,* 3468-3496.

18. Rausch, C.; Hoof, I.; Weber, T.; Wohlleben, W.; Huson, D. H. *BMC Evol. Biol.* **2007,** *7:* 78, doi:10.1186/1471-2148-7-78.

19. Nguyen, K. T.; Kau, D.; Gu, J. Q.; Brian, P.; Wrigley, S. K.; Baltz, R. H.; Maio, V. *Mol. Microbiol.* **2006,** *61,* 1294-1307.

20. Kopp, F.; Grunewald, J.; Malhert, C.; Marahiel, M. A. *Biochemistry* **2006,** *45,* 10474-10481.

21. Grunewald, J.; Sieber, S. A.; Malhert, C.; Linne, U.; Marahiel, M. A. *J. Am. Chem. Soc.* **2004,** *126,* 17025-17031.

22. Lakey, J. H.; Ptak, M. *Biochemistry* **1988,** *27,* 4639-4645.

23. Ball, L. J.; Goult, C. M.; Donarski, J. A.; Micklefield, J.; Ramesh, V. *Org. Biol. Chem.* **2004,** *2,* 1872-1878.

24. Straus, S. K.; Hancock, R. E. W. *Biochim. Biophys. Acta.* **2006,** *1758,* 1215-1223.

25. Ho, S. W.; Jung, D.; Calhoun, J. R.; Lear, J. D.; Okon, M.; Scott, W. R.; Hancock, R. E.; Straus, S. K. *Eur. Biophys. J.* **2008,** *37,* 421-433.

26. Muriah, J. K.; Pearson, A.; Silverman, J.; Palmer, M. *Biochim. Biophys. Acta.* **2011,** *1808,* 1154-1160.

27. Muriah, J. K.; Harris, J.; Taylor, S. D.; Palmer, M. *Biochim. Biophys. Acta.* **2012,** *1818,* 673-678.

28 Pogliano, J.; Pogliano, N.; Silverman, J. A. *J. Bacteriol.* **2012,** *194,* 4494-4504.

29. Silverman, J. A.; Perlmutter, N. G.; Shapiro, H. M. *Antimicrob. Agents Chemother.* **2003,** *47,* 2538-2544.

30. Allen, N. E.; Alborn Jr, W. E.; Hobbs Jr, J. N. *Antimicrob. Agents Chemother.* **1991,** *35,* 2639-2642.

31. Lewis, J. S.; Owens, A.; Cadena, J.; Sabol, K.; Patterson, J. E.; Jorgenson, J. H. *Antimicrob. Agents Chemother.* **2005,** *49,* 1664-1665.

32. Sauermann, R.; Rothenburger, M.; Graninger, W.; Joukhadar, C. *Pharmacology* **2008,** *81*, 79-91.

33. Tran, T. T.; Panesso, D.; Mishra, N. N.; Mileykovskaya, E.; Guan, Z.; Munita, J. M.; Reyes, J.; Diaz, L.; Weinstock, G. M.; Murray, B. E.; Shamoo, Y.; Dowhan, W.; Bayer, A. S.; Arlas, C. A. *mBio* **2013,** *4*, e00281-e00213.

34. Marti, V. H.; Sanchez, E. R.; Lieti, M. S.; Ribeiles, B.; Andreas, J. L. P. *Rev. Esp. Quimioterap* **2007,** *20*, 261-276.

35. Skiest, D. J. *J. Clin. Microbiol.* **2006,** *44*, 655-656.

36. Hirschwerk, D.; Ginocchio, C. C.; bythro, M.; Condon, S. *Infect. Control Hosp. Epidemiol.* **2006,** *27*, 315-317.

37. Kaatz, G. W.; Lundstrom, T. S.; Seo, S. M. *Int. J. Antimicrob. Agents* **2006,** *28*, 280-287.

38. Friedman, L.; Alder, J. D.; Silverman, J. A. *Antimicrob. Agents Chemother.* **2006,** *50*, 2137-2145.

39. Julian, K.; Kosowska-Shick, K.; Whitener, C.; Roos, M.; Labischinski, H.; Rubio, A.; Parent, L.; Ednie, L.; Koeth, L.; Bogdanovich, T.; Applebaum, P. C. *Antimicrob. Agents Chemother.* **2007,** *51*, 3445-3448.

40. Rubio, A.; Conrad, M.; Haselbeck, R.; Kedar, G. C.; Driver, V.; Finn, J.; Silverman, J. abstract C1-4179. *48th Annual ICAAC Meeting*, Washington, DC, October, 2008.

41. Rubio, A.; Conrad, M.; Haselbeck, R.; Kedar, G. C.; Driver, V.; Finn, J.; Silverman, J. Abstract C1-4180. *48th Annual ICAAC Metting*, Washington DC, October, 2008.

42. Dubrac, S.; Boneca, I. G.; Poupel, O.; Msadek, T. *J. Bacteriol.* **2007,** *189*, 8257-8269.

43. Wrinkler, M. E.; Hock, J. A. *J. Bacteriol.* **2008,** *190*, 2645-2648.

44. Fukushima, T.; Szurmant, H.; Kim, E. J.; Perego, M.; Hoch, J. A. *Mol. Microbiol.* **2008,** *69*, 621-632.

45. Hachmann, A. B.; Angert, E. R.; Helmann, J. D. *Anitmicrob. Agents Chemother.* **2009,** *53*, 1598-1609.

46. Cotroneo, N.; Harris, R.; Perlmutter, N.; Beveridge, T.; Silverman, J. A. *Antimicrob. Agents Chemother.* **2008,** *52*, 2223-2225.

47. Nguyen, K.; Ritz, D.; Gu, J. Q.; Alexander, D.; Chu, M.; Maio, V.; Brian, P.; Baltz, R. H. *Proc. Nat. Acad. Sci. U.S.A.* **2006,** *103,* 17462-17467.

48. Eggert, U. S.; Ruiz, N.; Falcone, B. V.; Branstrom, A. A.; goldman, R. C.; Silhavy, T. J.; Kahne, D. *Science* **2001,** *294,* 361-364.

49. Baltz, R. H. *Current Opinion in Chemical Biology* **2009,** *13,* 144-151.

50. Munoz-Price, L. S.; Lolans, K.; Quinn, J. P. *Clin. Infect. Dis.* **2005,** *41,* 565-566.

51. Jordan, S.; Hutchings, M. I.; Mascher, T. *FEMS Microbiol. Rev.* **2008,** *32,* 107-146.

52. Munita, J. M.; Tran, T. T.; Diaz, L.; Panesso, D.; Reyes, J.; Murray, B. E.; Arias, C. A. *Antimicrob. Agents Chemother.* **2013,** *57,* 2831-2833.

53. Arias, C. A.; Panesso, D.; McGrath, D. M.; Quin, X.; Mojica, M. F.; Miller, C.; Diaz, L.; Tran, T. T.; Rincon, S.; Barbu, E. M.; Reyes, J.; Roh, J. H.; Lobos, E.; Sodergren, E.; Pasqualini, R.; Arap, W.; Quinn, J. P.; Shamoo, Y.; Murray, B. E.; Weinstock, G. M. *N Eng J. Med.* **2011,** *365,* 892-900.

54. Munita, J. M.; Panesso, D.; Diaz, L.; Tran, T. T.; Reyes, J.; Wanger, A.; Murray, B. E.; Arias, C. A. *Antimicrob. Agents Chemother.* **2012,** *56,* 4354-4359.

55. Mishra, N. N.; Bayer, A. S.; Tran, T. T.; Shamoo, Y.; Mileykovskaya, E.; Dowhan, W.; Guan, Z.; arias, C. A. *PLoS One* **2012,** *7:e43958,* DOI: 10.1371/journal.pone.0043958.

56. Davlieva, M.; Zhang, W.; Arias, C.A.; Shamoo, Y. *Antimicrob. Agents Chemother.* **2013**, *57*, 289-296

57. Palmer, K.L.; Daniel, A.; Hardy, C.; Silverman, J.; Gilmore, M.S. *Antimicrob. Agents Chemother.* **2011**, *55*, 3345-3356.

58. Jones, T.; Yeaman, M. R.; Sakoulas, G.; Yang, S. J.; Proctor, R. A.; Sahl, H. G.; Schrenzel, J.; Xiong, Y. Q.; Bayer, A. S. *Antimicrob. Agents Chemother.* **2008,** *52*, 269-278.

59. Bayer, A. S.; Schneider, T.; Sahl, H. G. *Ann. N.Y. Acad. Sci.* **2013,** *1277,* 139-158.

60. Mishra, N. N.; Yang, S. J.; Sawa, A.; Rubio, A.; Nast, C. C.; Yeaman, M. R.; Bayer, A. S. *Antimicrob. Agents Chemother.* **2009,** *53,* 2312-2318.

61. Mileykovskaya, E.; Dowhan, W. *J. Bacteriol* **2000,** *182,* 1172-1175.

62. Kicia, M.; Janeczko, N.; Lewica, J.; Hendrich, A. B. *J. Med. Microbiol* **2012,** *61,* 520-524.

63. Barak, I.; Muchova, K.; Wilkinson, A. J.; O'Toole, P. J.; Pavlendova, N. *Mol. Microbiol.* **2008,** *68,* 1315-1327.

64. Kawai, F.; Shoda, M.; Harashima, R.; Sadaie, Y.; Hara, H.; Matsumoto, K. *J. Bacteriol.* **2004,** *186,* 1475-1483.

65. Zhang, T.; Muriah, J.K.; Tishbi, N.; Herskowitz, J.; Victor, R.L.; Silveman, J.; Uweumarenogie, S.; Taylor, S.D.; Palmer, M.; Mintzer, E.J. *Biol. Chem.* **2014**, *289,* 11584-11591

66. Dubinsky, L.; Krom, B. P.; Meijler, M. M. *Bioorg. Med. Chem.* **2012,** *20,* 554-570.

67. Robinette, D.; Neamati, N.; tomer, K. B.; Borchers, C. H. *Expert Rev. Proteomics* **2006,** *3,* 399-408.

68. Sumranjit, J.; Chung, S. J. *Molecules* **2013,** *18,* 10425-10451.

69. Das, J. *Chem. Rev.* **2011,** *111,* 4405-4444.

70. Vodovozova, E. L. *Biochmistry-Moscow* **2007,** *72,* 1-20.

71. Breslow, R. *Acc. Chem. Res.* **1995,** *28,* 146-153.

72. Breslow, R. *Acc. Chem. Res.* **1980,** *13,* 170-177.

73. Galardy, R. E.; Craig, L. C.; Jamieson, J. D.; Printz, M. P. *J. Biol. Chem.* **1974,** *249,* 3510-3518.

74. Dorman, G.; Prestwich, G. D. *Biochemistry* **1994,** *33,* 5661-5673.

75. Turro, N. *Modern Molecular Photochemistry;* Benjamin/Cummings: Menlo Park, CA, 1978.

76. Wagner, P. J. *Acc. Chem. Res.* **1971,** *4,* 168-177.

77. Wagner, P. J.; Park, B. S. *Adv. Photochem.* **1991,** 227-363.

78. Kotzyba-Hibert, F.; Kapfer, I.; Goeldner, M. *Angew. Chem. Int. Ed. Engl.* **1995,** *34,* 1296-1312.

79. Monti, S.; Camjoni, N.; Bortolus, P. *Photochem. Photobiol.* **1991,** *54,* 577-584.

80. Moore, G. G. I.; Harrington, J. K. *J. Med. Chem.* **1975,** *18,* 386-391.

81. Holt, A. D.; Yamashita, D. S.; Konialian-Beck, A. L.; Luengo, J. I.; Abell, A. D.; Bergsma, D. J.; Brandt, M.; Levy, M. A. *J. Med. Chem.* **1995,** *38,* 13-15.

82. Prestwich, G. D.; Dorman, G.; Elliot, J. T.; Marecak, D. M.; Chaudhary, A. *Photochem. Photobiol.* **1997,** *65,* 222-234.

83. Nakayama, H.; Hatanaka, Y.; Taki, M.; Yoshida, E.; Kanoaka, Y. *Ann. N.Y. Acad. Sci.* **1993,** *707,* 349-351.

84. Hatanaka, Y.; Sadakane, Y. *Curr. Top. Med. Chem.* **2002,** *2,* 271-288.

85. Gilchrist, T. L.; Rees, C. W. *Carbenes, Nitrenes and Arynes;* The Pitman Press: Bath, 1969.

86. Mueller, P. H.; Rondan, N. G.; Houk, K. N.; Harrison, J. F.; Hooper, D.; Willen, B. H.; Liebman, J. F. *J. Am. Chem. Soc.* **1981,** *103,* 5049-5052.

87. Perez, J. M. *J. Chem. Soc. Faraday Trans. 1* **1982,** *78,* 3509-3518.

88. Zhang, Y.; Burdzinski, G.; Kubicki, J.; Platz, N. S. *J. Am. Chem. Soc.* **2008,** *130,* 16134-16135.

89. Moss, R. A.; Lu, Z.; Sauers, R. R. *Tetrahedron Lett.* **2010,** *51,* 5940-5942.

90. Noller, B.; Poisson, L.; Maksimenka, R.; Bobert, O.; Fischer, I.; Mestdagh, J. M. *J. Phys. Chem.* **2009,** *113,* 3041-3050.

91. Noller, B.; Hemberger, P.; Fischer, I.; Alcaraz, C.; Garcia, G. A.; Soldi-Lose, H. *Phys. Chem. Chem. Phys.* **2009,** *11,* 5384-5391.

92. Staros, J. V. *TIBS* **1980,** *5,* 320-322.

93. Smith, P. A. S. *Nitrenes;* Wiley Interscience: New York, 1970.

94. Staros, J. V.; Bayley, H.; Standring, D. N.; Knowles, J. R. *Biochem. Biophys. Res. Commun.* **1978,** *80,* 568-572.

95. Cartwright, I. L.; Hutchinson, D. W.; Armstrong, V. W. *Nucleic Acids Res.* **1976,** *3,* 2331-2339.

96. Reiser, A.; Willets, F. W.; Terry, G. C.; Williams, V.; Marley, R. *Trans. Faraday Soc.* **1968,** *64,* 3265-3275.

97. Ruoho, A. E.; Kiefer, H.; Roeder, P. E.; Singer, S. J. *Proc. Nat. Acad. Sci. U.S.A.* **1973,** *70,* 2567-2571.

98. Kiehm, D. J.; Ji, T. H. *J. Biol. Chem.* **1977,** *252,* 8524-8531.

99. Eirich, J.; Orth, R.; Sieber, S.A. *J. Am. Chem. Soc.* **2011**, *133*, 12144-12153.

100. Speers, A.E.; Adam, G.C.; Cravitt, B.F. *J. Am. Chem. Soc.* **2003**, *125*, 4686-4687.

101. Huisgen, R. *1,3 Dipolar Cycloaddition Chemistry*; Wiley: New York, 1984.

102. Rostovtsev, V.V.; Green, J.G.; Fokin, V.V.; Sharpless K.B. *Angew. Chem. Int. Ed.* **2002**, *41*, 2596-2599.

103. Tornoe, C.W.; Christensen, B.G.; Meldal, M.J. *J. Org. Chem.* **2002**, *67*, 3057-3064.

104. Siedlecki, J.; Hill, J.; Parr, I.; Yu, X.; Morytko, M.; Zhang, Y.; Silverman, J.; Controneo, N.; Langanas, V.; Li, T.; Li, J.; Keith, D.; Shimer, G.; Finn, J. *Bioorg. Med. Chem. Lett.* **2003,** *13*, 4245-4249.

105. Silverman, J. A.; Mortin, L. I.; VanPraagh, A. D. G.; Li, T.; Alder, J. *Infect. Dis.* **2005,** *191,* 2149-2152.

106. Nakamura, I.; Nemoto, T.; Shiraiwa, N.; Terada, M. *Org. Lett.* **2009**, *11*, 1055-1058.

107. Siedlecki, J.; Hill, J.; Parr, I.; Morytko, M.; Yu, X.; Zhang, Y.; Silverman, J.; Contreoneo, N.; Laganas, V.; Li, T.; Li, F.; Kieth, D.; Shimer, G.; Finn, J. *Bioorg. Med. Chem. Lett.* **2003**, *13*, 4187-4191.

108. Siedlecki, J.; Hill, J.; Parr, I.; Yu, X.; Morytko, M.; Zhang, Y.; Silverman, J.; Contreoneo, N.; Laganas, V.; Li, T.; Li, F.; Kieth, D.; Shimer, G.; Finn, J. *Bioorg. Med. Chem. Lett.* **2003**, *13*, 4245-4249.

109. Muriah, J.K.; Harris, J.; Taylor, S.D.; Palmer, M. *Biochim. Biophys. Acta*. **2012**, *3*, 673-678.

110. Gooben, L.J.; Winkel, L.; Dohring, A.; Ghosh, K.; Paetzold, J. *Synlett.* **2002**, *8*, 1237-1240.

111. Yang, C.; Edsall Jr., R.; Harris, H.A.; Zhang, X.; Manas, E.S.; Mewshaw, R.E. *Bioorg. Med. Chem.* **2004**, *12*, 2553-2570.

112. Jubin, H.; Xu, B.; Hammond, G.B. *Org. Lett.* **2011**, *13*, 3450-3453.

113. Gopalan, B.; Lingham, V.S.; Thomas, A.; Vinodkumar, R.; Mukkanti, K. *Tetrahedron Lett.* **2008**, *49*, 4260-4264.

114. Batel, S.; Hahn, M.; Ahmed, W.; Becker, E.M.; Roelle, T.; Stasch, J.P.; Schlemmer, K.H.; Wunder, F.; Knorr, A.; Lang, D. *U.S. Pat. US2010/29772 A1*. **2010**.

115. Kimura, H.; Tayama, E. *Angew. Chem. Int. ed.* **2007**, *46*, 8869-8871.

116. Sharma, G.V.M.; Reddy, K.L.; Reddy, J.J.; *Tetrahedron Lett.* **2006**, *47*, 6537-6540.

117. Tam, J.P.; Reimen, M.W.; Merrifield, R.B. *Peptide Research.* **1988**, *1*, 6-18.

118. Wang, N.; Huang, K.; Wang, L.; *Polym. Bull.* **2011**, *67*, 1569-1581.

119. Meddour, A.; Courtieu, J. *Tetrahedron Asymmetry.* **2000**, *11*, 3635-3644.

120. Klyatskaya, S.V.; tretyakov, E.V.; Vasilevsky, S.F. *Russ. Chem. Bull. Int. Ed.* **2002**, *51*, 128-134.